Charles University in Prague
Faculty of Mathematics and Physics

DIPLOMA THESIS

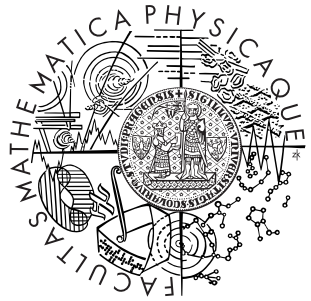

Martin Varga

The study of of DC and AC characteristics of polyaniline prepared by various ways

Department of Macromolecular Physics

Supervisor: RNDr. Jan Prokeš, CSc.

Study program: Physics of Condensed Matter

2011

Univerzita Karlova v Praze
Matematicko-fyzikální fakulta

DIPLOMOVÁ PRÁCE

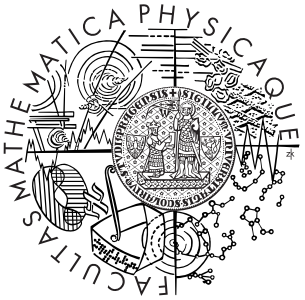

Martin Varga

Studium stejnosměrných a střídavých charakteristik polyanilinu v závislosti na technologii přípravy

Katedra makromolekulární fyziky

Vedoucí diplomové práce: RNDr. Jan Prokeš, CSc.

Studijní program: Fyzika kondenzovaných látek a materiálů

2011

First of all, I would like to express my very deep gratitude to my supervisor RNDr. Jan Prokeš, CSc. for leading me through both, the experimental and the theoretical aspects of my work. Many thanks also to my consultants Doc RNDr. Jan Nedbal, CSc. for his help, especially in the field of the dielectric spectroscopy and the AC conductivity, and RNDr. Ivo Křivka, CSc. for his fruitfull discussions and help in the area of the experiment automation. I am also indebted to RNDr. Jaroslav Stejskal, CSc. and his colleagues at the Institute of Macromolecular Chemistry Academy of Sciences of the Czech Republic for the prepared samples and the chemistry insight. I am gratefull to Mrs. Anna Aulická for the preliminary measurements and Mgr. Jana Kazíková for the language corrections. The last but not the least, I am very thankfull to all my colleagues, friends and family as without their support neither my studies nor this thesis would have never come to this point.

The results of this work contribute to the several published papers and were also presented at two poster sessions. The financial support from grant n. SVV2010261305 and the research plan MSM0021620834 financed by the Ministry of Education, Youth and Sports of the Czech Republic is fully acknowledged.

I declare that I carried out this master thesis independently, and only with the cited sources, literature and other professional sources.

I understand that my work relates to the rights and obligations under the Act No. 121/2000 Coll., the Copyright Act, as amended, in particular the fact that the Charles University in Prague has the right to conclude a license agreement on the use of this work as a school work pursuant to Section 60 paragraph 1 of the Copyright Act.

Prohlašuji, že jsem tuto diplomovou práci vypracoval samostatně a výhradně s použitím citovaných pramenů, literatury a dalších odborných zdrojů.

Beru na vědomí, že se na moji práci vztahují práva a povinnosti vyplývající ze zákona č. 121/2000 Sb., autorského zákona v platném znění, zejména skutečnost, že Univerzita Karlova v Praze má právo na uzavření licenční smlouvy o užití této práce jako školního díla podle §60 odst. 1 autorského zákona.

V Praze dne 14.4.2011 Martin Varga

Název práce: Studium stejnosměrných a střídavých charakteristik polyanilinu v závislosti na technologii přípravy
Autor: Martin Varga
Katedra: Katedra makromolekulární fyziky
Vedoucí diplomové práce: RNDr. Jan Prokeš, CSc.
e-mail vedoucího: jprokes@semi.mff.cuni.cz

Abstrakt: Našim cílem v předložené práci je provést a vyhodnotit stejnosměrné a střídavé charakteristiky materiálů založených na polyanilinu. K dosažení tohoto cíle bylo použito několika experimantálních metod a zařízení. Také je nastíněn teoretický úvod do problematiky. Vlastním jádrem práce je zkoumání závislostí elektrické vodivosti na teplotě a tlaku a také stárnutí dvou systémů (kompozitů) s ohledem na různé způsoby přípravy, např. různé dopanty a jejich molární koncentrace, původ a obsah anorganické složky a způsob polymerizace. Rovněž je diskutována shoda s teoretickými modely.

Klíčová slova: vodivé polymery, polyanilin, střídavá a stejnosměrná vodivost, kompozity

Title: The study of of DC and AC characteristics of polyaniline prepared by various ways
Author: Martin Varga
Department: Department of Macromolecular Physics
Supervisor: RNDr. Jan Prokeš, CSc.
Supervisor's e-mail address: jprokes@semi.mff.cuni.cz

Abstract: Our aim in the present work is to provide and evaluate AC and DC characteristics of the polyaniline based materials. Different experiemtal techniques and devices have been used to achieve this goal. An introduction to the theoretical concepts of conductivity is given as well. The core of this thesis is an investigation of temperature and low pressure dependences, as well as the ageing effects for two systems (composites) in respect of the different preparation conditions such as dopants and their molar concentration, origin and the content of inorganic component and the way of polymerisation. An agreement with theoretical models is discussed.

Keywords: conducting polymers, polyaniline, AC and DC conductivity, composites

Contents

List of Symbols and Abbreviations

α, β	parameters of phenomenological dielectric function
α_L	reciprocal value of localized wave function decay
α_ρ	temperature coefficient of resistivity
$\delta_{i,j}$	Kronecker delta
ϵ^*, ϵ_t^*, ϵ',ϵ''	complex permittivity (dielectric function),the total complex permittivity, real and imaginary part of the complex permittivity
ϵ_0	permittivity of free space
ϵ_s, ϵ_∞	$lim_{\omega\to 0}\epsilon'(\omega)$, $lim_{\omega\to\infty}\epsilon'(\omega)$
η	volume fraction of conducting islands in insulating matrix
γ	exponent in VRH-like models
$\hbar$	Planck constant
$\mathbf{k}$	wave vector
$\mathbf{P}$	polarisation
$\mathbf{r}$, $\mathbf{R}$	elecron resp. nucleus position
μ_n, μ_p	electron, hole mobility
ν	technical frequency
ω	angular frequency
ω_c	critical (σ_{AC} onset) frequency
ω_m	frequency of loss peak maximum
ω_{ph}	phonon frequency
ϕ, ϕ_C	content of conductive phase, its critical value
ρ	electrical resistivity
σ, σ_{DC}	electrical conductivity, DC electrical conductivity

σ^*, σ', σ''	complex electrical conductivity, real and imaginary part of complex conductivity
τ	relaxation time
ξ	coupling constant of electron-phonon interaction
A	cross-sectional area
C	capacitance
c_1, c_2	parameters of Williams-Landel-Ferry equation
$c_{n,s}$, $c^\dagger_{n,s}$	fermionic creation and anihilation operators
D	dimensionality of system
e	electric charge of electron
E, W	energy
E_a	activation energy of process
E_H	hopping energy barrier
F	correction factor in four-probe method
f	electron distribution function
g	geometrical factor in heterogeneity model
$g(\tau)$	distribution of relaxation times
H	Hamiltonian
I	electric current
K	spring constant
k_B	Boltzmann constant
l	length
m, M	electron resp. nucleus mass
M^*	complex electrical modulus
M_{acid}	molar concentration of acid
n, p	electrons, holes concentration
$N(E_F)$	density of states at Fermi level
p	percolation conductivity exponent
R	electrical resistance
R_H	hopping distance between localized states

s	exponent in 'universal' AC conductivity power law
T	temperature
t	time resp. thickness
t_0	hopping integral
T_0,T_1	characteristic temperature parameters for soft-exponential models
U	voltage
u	junction volume in FIT model
u_n	displacement of n^{th} group in polymer chain
V_0, E_0	height of potential barrier and related electrostatic energy in FIT model
W_H	polaron activation energy
Z	electric impedance
$\mathbf{D}$	electric displacement
$\mathbf{E}$	electric field
$\mathbf{j}$	electric current density
AC	acetic acid
AC/DC	alternating/direct current
Ag	silver
ARH	Arrhenius thermally activated process
CELT	charging energy limited tunneling
CL,IV,BF	montmorillonite: Cloisite, Ivančice, Belle Fourche
CP(s)	conducting polymer(s)
CSA	camphorsulphonic acid
FA	formic acid
FIT	fluctuation-induced tunneling
FTIR	Fourier transform infrared spectroscopy
M-I	metal-insulator (transition)
MMT	montmorillonite
MSA	methanesulphonic acid
PA	polyacetylene

PANI	polyaniline
PPY	polypyrrole
Q1D	quasi-one-dimensional
SFA	aminosulphonic acid
SSH	Su-Schrieffer-Heeger model
TEM	transmittion electron microscope
TGA	thermal gravimetric analysis
TSA	toluenesulphonic acid
VdP	four-probe method in Van der Pauw configuration
VRH	variable range hopping

And I gave my heart to know wisdom, and to know madness and folly: I perceived that this also is vexation of spirit. For in much wisdom is much grief: and he that increaseth knowledge increaseth sorrow.

Ecclesiastes 1:17-18

Preface

The knowledge of electrical properties of materials are essential for human beings as it enables further development as well as the production of a huge variety of everyday life usage devices based on the conducting, the semiconducting and/or the insulating materials. It was a long time ago that the 'classical' inorganic conductors such as copper, silver, platinum and semiconductors mainly silicon were widely used for these applications and their properties are more or less well understood nowadays. On the other hand, polymers were known to the mankind as insulator for many decadess. The situation changed dramatically when conducting polymers (CPs) were re-discovered in 1970s in terms of electrical conductivity. The importance of this discovery was confirmed by the Nobel prize for Chemistry in 2000 when three discoverers - A.J. Heeger, A.G. MacDiarmid and H. Shirakawa were awarded [1]. Conducting polymers show both metallic and semiconducting behaviour covering a full range of room temperature conductivities provided by 'classical' metals or semiconductors [2]. That is why these materials promise a variety of implementations in industry. According to one of the 'fathers' of conducting polymers, A.J. Heeger, they also brought the opportunity to deal with fundamental problems in quantum chemistry (understanding of π bonds) and condensed matter physics (metal-insulator transition, Anderson localization, etc.) as well [1]. No doubt, all these reasons encouraged plenty of research in the past and we believe it is still worth going on with further investigation.

This thesis composes of five chapters. The general theoretical background of conductivity and conducting polymers is introduced in chapter 1 and together with chapter 2, where basic experimental methods for electrical properties measurements are explained, give a theoretical framework essential for further work. The own part of this thesis is experimental with its aim of characterisation of materials prepared at Institute of Macromolecular Chemistry of Academy of Sciences of Academy of Sciences of the Czech Republic, and begins in chapter 3 with description of used techniques and devices and goes on with experimental results and their own evaluation in chapter 4. Finally, chapter 5 concerns conclusions of this work.

Chapter 1

Theoretical background of electrical conductivity and conducting polymers

In this chapter we are trying to provide an overview of physics behind the electrical conductivity and the dielectric response of materials. We start with basic definitions of the conductivity, subsequently we turn our attention to the electronic structure and transport mechanisms in 'classical' metals and semiconductors that are very well understood nowadays and serve as the basics for an understanding of conducting polymers that follow. The end of this theoretical chapter is dedicated to polyaniline as an example of conducting polymers but at the same time the base of our experimental study. In this theoretical review we are providing only basic, however fundamental knowledge essential for a better understanding of the topic without any details and derivations which can be found elsewhere (i.e. in references listed at the end of this work).

1.1 A short introduction to conductivity

1.1.1 DC conductivity

The electrical conductivity belongs to a group of transport phenomena and can be understood as reaction of system to the applied external electric field $\mathbf{E}$ in order to restore the thermodynamic equilibrium state through the electric current density $\mathbf{j}$. When the applied fields are low enough, a linear response of the system occurs. In our case of the electrical conductivity σ it leads to the well-known Ohm's law:

$$\mathbf{j} = \sigma \mathbf{E} \tag{1.1}$$

where σ in principle can be a tensor of the second order. But in the case of the isotropic conductivity it is just a constant providing relationship between the applied

external electric field (cause) and the electric current density (consequence). The expression (1.1) thus can be considered as a definition of the electrical conductivity. Its units are Siemens per meter S/m but practically the most often used unit is S/cm. Its reciprocal value defines the electrical resistivity ρ with units Ωm what is very often a better way for expressing the relation between the current and the applied field. It can be related to the dimensions of material:

$$\rho = \frac{1}{\sigma} = RA/l \tag{1.2}$$

with the resistance R, the cross-sectional area A and the length l. From the electric point of view materials can be classified as metals with $\frac{d\sigma}{dT} < 0$ and semiconductors with $\frac{d\sigma}{dT} > 0$. Other classification by room temperature values distinguishes between conductors with σ higher than 10^3 S/cm, insulators with σ about 10^{-12} S/cm and semiconductors somewhere in between [3]. Certainly, these borders are not strict and can differ from author to author. Maybe physically the best classification is in terms of the band theory (which will be described later) where metals typically have their Fermi level in conduction band while for insulators (semiconductors) the Fermi level lies in the energy gap between the occupied valence band and the empty conduction band. A distinction between semiconductors and insulators is rather artificial, in the width of the band gap.

1.1.2 AC conductivity and dielectric response

Up to now we have considered the electric field as frequency (time) independent but one can also be interested in dynamic properties or response of a material to the applied frequency dependent electric field, for instance, $\mathbf{E}(\omega) = \mathbf{E}_0 e^{i\omega t}$. Then the conductivity becomes frequency dependent as well, the expression (1.1) is now in the form:

$$\mathbf{j}(\omega) = \sigma^*(\omega)\mathbf{E}(\omega) \tag{1.3}$$

again with σ^* generally taken as a tensor but now even a complex number. The situation is becoming more complicated. In general, the interaction of electromagnetic field with matter is macroscopically described by the Maxwell's equations and there are as free mobile charge carriers (electrons, ions) with a contribution to the conductivity as well as bound charges with a resonance response (optical frequencies) and relaxation processes linked with the polarisation $\mathbf{P}$. The response of a material is given by electric displacement $\mathbf{D}$:

$$\mathbf{D} = \epsilon^* \epsilon_0 \mathbf{E} \tag{1.4}$$

which is related to the electric field through the complex permittivity ϵ^* and the permittivity of free space ϵ_0. The real part ϵ' of ϵ^* expreses the energy reversibly stored in the system while the imaginary part ϵ'' reflects energy dissipated. The macroscopic polarisation, what is a summation over all microscopic dipole moments, then reads:

$$\mathbf{P} = \mathbf{D} - \mathbf{D_0} = (\epsilon^* - 1)\epsilon_0 \mathbf{E} \tag{1.5}$$

The microscopic dipole moments can be either induced by the external field (e.g. elecronic cloud or atomic polarisation) or permanent giving arise to the so called orientational polarisation. There is also a contribution of the DC conductivity to the total complex permittivity $\epsilon_t^*(\omega)$:

$$\epsilon_t^*(\omega) = \epsilon^*(\omega) + i\frac{\sigma_{DC}}{\omega}\epsilon_0 \tag{1.6}$$

where only the imaginary part is affected by the pure ohmic electronic conductivity.

It can be shown from the Maxwell's equations that the complex conductivity is related to the complex permittivity by a relation:

$$\sigma^*(\omega) = i\omega\epsilon_0\epsilon^*(\omega) \tag{1.7}$$

and both carry the same physical information. The third alternative is the so called electric modulus M^* which holds:

$$M^*(\omega)\epsilon^*(\omega) = 1 \tag{1.8}$$

We can certainly work in a time domain and describe the time t dependences of physical variables but practically the frequency domain is more appropriate and both results are related by the one-sided Fourier transformation, e.g.:

$$\epsilon^*(\omega) = \epsilon_\infty - \int_0^\infty \frac{d\epsilon(t)}{dt}e^{-i\omega t}dt \tag{1.9}$$

with a high frequency limit ϵ_∞ reflecting very fast polarisation processes (atomic and electronic cloud polarisation). More details can be found for instance in ref. [4]

In general, the conductivity representation is preferred in physics of (semi)conductors where the transport properties are the object of an interest and the frequency dependence of real part of complex conductivity is usually investigated. While permittivity representation is successfully used when material is dielectric, its response on the electric field is mainly due to the polarisation and the relaxation mechanisms are of interest.

1.1.3 Electronic structure and charge transport in metals and semiconductors

In order to explain the conduction mechanisms in solids, one needs to know the properties and the behaviour of charge carriers (electrons, ions). Undoubtedly, the first successfull theory at least partly explaining the conductivity in metals was the Drude's theory giving the first and an important insight into this field of study. In

fact, it was a classical kinetic theory of electron gas where each atom donates at least one electron in common. This electron gas is colliding with positive ions in metallic lattice and electrons gain the drift velocity from the applied external electric field **E**. There can be a formula for the electrical conductivity derived and reads:

$$\sigma = \frac{ne^2\tau}{m} \tag{1.10}$$

with n as a number of electrons, τ the relaxation time (time between two collisions), e the electric charge of electron and m the mass of electron. Its temperature dependence could be estimated as $\sigma \sim T^{-1/2}$. Furthermore, within this free electron model also the frequency dependent conductivity can be understood:

$$\sigma(\omega) = \frac{\sigma(0)}{1 + i\omega\tau} \tag{1.11}$$

with $\sigma(0)$ given by eqn. (1.10). Despite of the partial success of this approach, the problem with the temperature dependence is obvious, moreover this theory totally failed in the heat capacity explanation. A step forward was achieved by the use of the quantum mechanics which is nowadays considered as an essential, and even a superior approach.

The understanding of the conductivity can not do without a deep knowledge of the electronic structure. That is given within quantum physics by the solution of the Schrödinger equation with the many-body Hamiltonian H concerning electron-electron, ion-ion and electron-ion interactions:

$$\begin{aligned} H = -\frac{\hbar^2}{2m}\sum_i \Delta_i - \frac{\hbar^2}{2M}\sum_I \Delta_I + \frac{1}{2}\sum_{i\neq j}\sum_j \frac{e^2}{4\pi\epsilon_0|\mathbf{r_i} - \mathbf{r_j}|} + \\ + \frac{1}{2}\sum_{I\neq J}\sum_J \frac{Z^2e^2}{4\pi\epsilon_0|\mathbf{R_I} - \mathbf{R_J}|} - \sum_i\sum_J \frac{Ze^2}{4\pi\epsilon_0|\mathbf{r_i} - \mathbf{R_J}|} \end{aligned} \tag{1.12}$$

with the Planck constant $\hbar$, m and $M$the mass of electron resp. nucleus, **r** and **R** the position of electron resp. nucleus and Ze the electric charge of nucleus. This many-body problem contains required information but is very difficult (if not impossible) to solve and different approximations had to be introduced. To sum them up:

- the separation of nuclei and electrons motion provided by the so called Born-Oppenheimer adiabatic approximation
- the reduction of the many-electron wave-function into the set of one-electron Schrödinger equations done by self-consistent methods such as Haartree, Haartree-Fock approximations or density functional theory

The later simplification is due to the electron-electron interactions one has to deal with and despite of this crude approximation they generally give satisfactory results. On the other hand with reduction to one-electron problem one looses information

about the 'many-body' effects due to e.g. electron-phonon interactions.

For the one-electron problem there were several methods proposed to obtain a solution. First of all, in the case of crystalline materials (metals, some semiconductors) that have a periodic structure it was noticed interesting property of periodic potential in Hamiltonian giving arise to the so called Bloch theorem which states that the electronic wave function is modulated by the periodic function providing the translational invariance in respect of vectors of the crystal lattice. Moreover, due to the large number of atoms in material discrete energy levels are replaced with a quasi-continuous spectrum. Calculating energies of states $E(k)$ in respect to the wave vectors k one gets a band structure what is a corner stone for dynamical properties such as the electrical conductivity. These bands can overlap or be separated by a gap. The zeroth approximation in this approach is the model of free electrons where electrons move in constant potential. The solution is analogous to motion of free electrons within the Sommerfeld model giving energy dispersion:

$$E(k) = \frac{\hbar^2 k^2}{2m} \tag{1.13}$$

The bands are parabolic and the electronic states are extended over a crystal. More realistic is the nearly free electron model based on the perturbation theory and is valid for small deviations from a constant potential. Another option might be, when the previous model fails, the tight binding model based on the idea of the strong atomic potentials or their linear combination near lattice points. Again it gives a band structure. Since this model rather fails between the ionic cores where a plane wave is expected, the combination of them both is often considered such as augmented plane waves, orthogonalised plane waves or the Green's function approach. More details are e.g. in ref. [5, 6]

Until now it was a typical procedure for the periodic potentials, but what if the heights of potential wells or the atomic positions are randomly distributed? This would bring some disorder to the system and to describe the situation, Anderson suggested the Hamiltonian of the system in the second quantisation formalism in the form of the Wannier states and the tight binding model with local energy W_n:

$$H = W_n \delta_{n,n'} + V_{n,n'} \tag{1.14}$$

For the cases where the intersite potential $V_{n,n'}$ is not zero and varies among states so called localization becomes important. It is defined as the unite probability (certainty) that with time going to infinity one finds a state in its initial state [6]. The localization of the charge carriers plays a crucial role in electrical conductivity for disordered systems (such as conducting polymers).

With the basic picture of the electronic band structure in solids one can go on with dynamics. The reaction of Bloch electrons on the external applied field depends on their band structure which is different for insulators/semiconductors and metals:

- in semiconductors there are either completely full or empty bands thus there are no currents (at least for small fields, otherwise a dielectric breakdown can occur as tunnelling of electrons from valence to a conduction band)
- in metals Fermi energy lies within a band, which is only partly filled, giving arise to the possibly huge currents which are only compensated by the scattering (otherwise the conductivity would be infinite).

The scattering in solids can have various origin e.g. impurities and defects in the crystal structure or phonons. The first one is often treated within Born approximation and is temperature independent, giving arise to the residual resistivity ρ_r even at zero temperature, the second one gives the temperature dependent resistivity $\rho(T)$ which vanishes at $T = 0$. These two different mechanisms are roughly additive what is known as the Matthiesen's rule.

The dynamic properties of metals and semiconductors are often successfully described by Boltzmann transport equation in terms of a total variation of the electron distribution function $f(\mathbf{r}, \mathbf{k}, t)$ where external fields and internal collisions are present:

$$\frac{df(\mathbf{k})}{dt} = \frac{\partial f(\mathbf{k})}{\partial t} + \left(\frac{df(\mathbf{k})}{dt}\right)_{fields} - \left(\frac{df(\mathbf{k})}{dt}\right)_{collisions} \tag{1.15}$$

which is very difficult to solve and the relaxation time approximation, where the collision term reflects the relaxation process of an equilibrium restoration after the removal of external fields, is a standard approach. Within this framework a temperature dependence for electrical conductivity can be derived. For metals the resistivity point of view is convenient and there is the power law $\sim T^5$ at very low temperatures, changing to the famous linear dependence:

$$\sigma^{-1}(T) = \rho(T) = \rho_r(1 + \alpha_\rho(T - T_r)) \tag{1.16}$$

with the temperature coefficient of resistivity α_ρ. The temperature dependence of conductivity in semiconductors is determined by the charge carriers concentration and their mobility temperature dependence:

$$\sigma(T) = e(n(T)\mu_n(T) + p(T)\mu_p(T)) \tag{1.17}$$

where n resp. p is the charge carriers concentration of electrons resp. holes, that can be intrinsic or come from doping. Their mobility is influenced by the scattering processes such as the impurity scattering with its $\sim T^{3/2}$ dependence or the phonon scattering with $\sim T^{-3/2}$ and this can result in different dependences but for high temperatures it often holds:

$$log\, \sigma(T) \sim -\frac{1}{T} \tag{1.18}$$

More details are far away behind the scope of this thesis and can be find elsewhere (e.g. [5,6]), nevertheless we believe that all these introduced basic ideas are important for the next step towards conducting polymers, in spite of the fact that these results derived from the Boltzmann transport theory are not valid in disordered materials, where this approach fails.

1.2 Conducting polymers

1.2.1 General overview

After years of interdisciplinary research in order to explain the behaviour of conducting polymers, scientists have agreed on some fundamental properties, although until now many challenges and open questions remain to be answered. The fundamentals about CPs can be found e.g. in ref. [1,3,7,8] but we are giving a brief overview below as well.

The reason why there are such materials showing the electrical conductivity in a family of polymers is that they are conjugated polymers. It means that each carbon atom contains π electron which does not take part in sp^2 hybridization (and does not form σ bonds). Some examples of their chemical structure are shown at figure 1.1.

(a) polyacetylene (PA)

(b) polypyrrole (PPY)

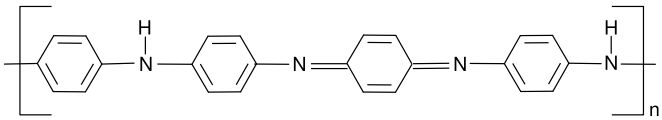

(c) polyaniline (PANI)

Figure 1.1: Chemical structure of some conducting polymers.

Since these π electron wave functions can overlap, they should form π band which is ideally half-filled (as each carbon atom has only one π electron in its molecular orbital). If this was true, conducting polymers would be perfect metals, but since they are one dimensional (1D) structures, this configuration is unstable due to electron-lattice interactions (so called Peierls instability of 1D metals) or electron-electron interactions. It means that an energetically favourable state is in the so called dimerized state where double and single bonds are alternating what expresses a symmetry breaking. For polyacetylene (PA) there are two equivalent phases and each stands for the minimum of potential. Because they are both energetically equivalent, the ground state is called degenerate. For the rest of polymers there are non-degenerate ground states with one global energy minimum. In the band terminology it means that there are two bands: the occupied (valence) π band and the empty (conduction) π^* band with the energy gap E_g determined by a molecular structure [9].

Due to the charge localization and the existence of the energy gap between the valence and the conduction band, for the electronic transport are responsible quasiparticles of mid-gap energy: solitons, polarons and bipolarons. Solitons in general are considered as the solutions of the nonlinear differential equations, in the condensed matter physics often sine-Gordon equation, providing a non-dispersing wave behaviour [10]. But the concept of solitons in CPs can be viewed clearly in PA structure where it is considered as bond alternation distortion giving rise to electronic state in energy gap. In this case the charge of an electron is compensated by the carbon nucleus and it is called neutral soliton. When a soliton is carring an electric charge we are dealing with a charged soliton. In this terminology polaron is a quasiparticle formed by neutral and charged soliton and analogously, two charged solitons form bipolaron [3].

The intrinsic concentration of mid-gap states is naturally low and some additional charge carriers have to be added. The injection of charge carriers, so-called doping (in analogy to 'classical' inorganic semiconductors), is usually performed. There are several ways how to do it:

- chemical doping by charge transfer - through the redox chemistry: oxidation (p-type doping) and reduction (n-type doping); it is efficient and straightforward allowing permanent doping; it is sufficient for fully doped materials
- electrochemical doping - in order to achieve a homogeneously moderately doped CP; a doping level is controlled by an applied voltage
- photo-doping - local oxidation/reduction by a photon absorption followed by a charge separation into free electrons and holes; this process competes with the recombination and provides temporary doping
- charge injection from metal electrode - electrons and holes are injected into CP, but there are no counter-ions; it provides temporary doping

Even if doping provides charge carriers in the polymer chain, the theoretical description is still far away from, for example, the classical band theory for semiconductors mainly due to:

+ a disorder typical for polymers which cause localization and even heavy doping does not lead to metalic structure
+ a deep interconnection between the chemical and the electronic structure - the elementary excitations involve lattice relaxation around electrons and holes what leads to thier self-localization and gives arise to quasiparticles: solitons, polarons and bipolarons
+ correlations between electrons - the Coulomb electron-electron and the electron-hole interactions - the origin of excitons (the neutral electron-hole bound states).

In general, one can consider the electronic structure of CPs in terms the of quasi-1D tight binding approximation providing π electron transfer integral to delocalize along the polymeric chain while the disorder and the Coulomb interaction tend to electron localization [1]. Within this framework known as the SSH (Su-Schrieffer-Heeger) model and using a formalism of the second quantisation[1] the Hamiltonian was suggested and for polyacetylene has the form [7]:

$$H_{SSH} = H_\pi + H_{\pi-ph} + H_{ph} = -t_0 \sum_{n,s} (c^\dagger_{n+1,s} c_{n,s} + c^\dagger_{n,s} c_{n+1,s}) +$$

$$+\xi \sum_{n,s} (u_{n+1} - u_n)(c^\dagger_{n+1,s} c_{n,s} + c^\dagger_{n,s} c_{n+1,s}) + \sum_n \frac{p_n^2}{2M} + \frac{K}{2} \sum_n (u_{n+1} - u_n)^2 \quad (1.19)$$

where the first term expresses hopping (t_0 hopping intergral) of π electrons along the chain, the second term stands for the electron-phonon interaction with the coupling constant ξ and u_n as displacement of n^{th} group and the last term is a standard phonon Hamiltonian with p_n as momentum, M mass of the group and K spring constant. To deal with the Coulomb interactions, the electron-electron Hamiltonian should be added and also some generalisation is required for systems with weakly lifted ground state degeneracy.

1.2.2 Transport mechanisms in DC conductivity

The electric charge transport depends strongly on the electronic structure of a material. Both the metallic and the semiconducting behaviour can be achieved depending on the preparation process. Several models and theoretical descriptions were suggested and widely used for the experimental data evaluation. A brief summary of them can be found in ref. [2], thera are also mentioned some basic ideas below. When CP falls into the metallic side there is a highly anisotropic quasi-one-dimensional metallic transport along the backbone chains which is limited by the phonon scattering with frequency ω_{ph} but for these phonons large temperatures are needed, the scattering is so called freezed, thus there should be a large room temperature conductivity of CPs in comparison to the classical metals. This model leads to the following temperature dependence [11]:

$$\sigma(T) = \sigma_0 exp\left(\frac{\hbar\omega_{ph}}{k_B T}\right) \quad (1.20)$$

where the pre-exponential factor is almost temperature independent against the exponential part. Because CPs are naturally strongly disordered they often fall into the insulating or the transition region. Near M-I transition there is the typical power law temperature dependence of conductivity:

$$\sigma(T) \sim T^\beta \quad (1.21)$$

[1] $c_{n,s}$ and $c^\dagger_{n,s}$ as fermionic creation and anihilation operators

For the semiconducting part there were several models taken from the disorder semiconductors physics that successfully describe the charge transport and its temperature dependence. As we mentioned before, a disorder causes the charge carrier localization (the Anderson localization). For this disordered materials conductivity is related mainly to thermally excited carriers and its dependence is in the form of eqn. (1.18). But the transport can be also due to hopping (the phonon-assisted tunneling) of carriers between the localized states. For instance, where the condition $\alpha_l R_H \gg 1$ is fullfilled, the hopping distance R_H is much greater than the distance $1/\alpha_L$ of the localized wave function decay, the nearest-neighbour hopping occurs with the temperature behaviour given by:

$$\sigma = \sigma_0 exp\left(-\frac{E_H}{k_B T}\right) \tag{1.22}$$

with the hopping energy barrier E_H, and the pre-exponential factor σ_0:

$$\sigma_0 = 2e^2 R_H^2 \nu_{ph} N(E_F) exp(-2\alpha_L R_H) \tag{1.23}$$

where e is the charge of electron and $N(E_F)$ is the density of states at the Fermi level. Where $\alpha_l R_H \geq 1$, rather hopping to the most favourable state is preffered known as the variable range hopping (VRH) leading to the temperature dependence:

$$\sigma(T) = \sigma_0 exp\left[-\left(\frac{T_0}{T}\right)^{\gamma}\right] \tag{1.24}$$

with slightly dependent σ_0 similar to the previous one given by eqn. (1.23) and parameter T_0:

$$T_0 = \frac{24\alpha_L^2}{\pi k_B N(E_F)} \tag{1.25}$$

and the exponent γ depending on the dimensionality D of the system:

$$\gamma = \frac{1}{1+D} \tag{1.26}$$

It should be noted that the original value for γ was 1/4 proposed by Mott [12]. Other coefficients were derived later, e.g. 1/2 when the Coulomb interaction was accounted [13] or even the coefficient 2/5 and 1/3 related to the impurity concentration and the impurity interaction [14]. It can be noticed that for 1D VRH or better Q1D VRH again $\gamma = 1/2$ is obtained. Moreover, this behaviour is valid mainly at low temperatures and to determine the process a wider temperature interval should be investigated [3].

A principally different approach can be chosen, that has its origin in composites (granular metals in insulating medium [15]), when there are regions with the extended electronic states, the so called 'metallic islands', separated by the insulating barriers. A charge is then transported through the electron tunnelling. When the metallic areas are sufficiently large, so that the thermal activated tunnelling accross

the barrier is not needed, because the wave functions overlap, then the voltage fluctuations greatly enhance the electron tunnelling giving rise to the so called fluctuation-induced tunnelling (FIT) with its temperature dependence for the simplified case of the parabolic barriers of junction [16]:

$$\sigma(T) = \sigma_0 exp\left(-\frac{T_1}{T+T_0}\right) \tag{1.27}$$

with again the almost temperature independent pre-exponential factor reflecting an intrinsic conductivity of the metallic islands and parameters T_1 and T_0 related to the geometry of junction as its volume u and the height of a potential barrier V_0 with the electrostatic charging energy E_0:

$$T_0 = \frac{4\sqrt{2}uE_0^2\hbar\epsilon\epsilon_0}{k_B\sqrt{mV_0}} \tag{1.28}$$

$$T_1 = \frac{uE_0^2 4\pi\epsilon\epsilon_0}{k_B} \tag{1.29}$$

For temperatures $T \ll T_0$ transport becomes temperature independent and for $T \gg T_0$ eqn. (1.27) changes to the thermally activated transport given by eqn. (1.18). When the conductive regions are not large enough and the electrostatic charging energy is higher than k_BT then the electronic tunneling through insulating material leads to a formula identical with eqn. (1.24) and exponent $\gamma = 1/2$ [17]. This model also provides an explanation for other exponents in the terms of the low and the infinity temperature limits. An analogous model more suitable mainly for CP taking into account the dopants as bridges for the tunneling (providing a polaronic cluster stability) was proposed by Zuppiroli et al. [18] where the conduction takes place due to the correlated hopping between polaronic clusters and the main barrier is due to the charging energy often referred as the charging energy limited tunneling (CELT). Again, this model gives the temperature dependence in the form of eqn. (1.24) with exponent 1/2 and parameter T_0 related to charging energy, grains sizes and distances.

It should be noted that VRH like models suppose a homogeneous disorder while CELT models rather a heterogeneous disorder and for many systems granularity or the heterogeneous models are essential for the explanation of experimental results and it seems that the granularity plays a crucial role in all CP systems but the relationship between the electronic and the structural heterogeneity is a complex question which keeps remaining opened [19]. Another approach is suggested by Kaiser [2] which considers linear series of different even homogeneous models providing thus heterogeneity. The contribution of different mechanisms is weighted by their geometrical factors g_i:

$$\sigma(T) = \sum_i g_i\sigma_i(T) \tag{1.30}$$

As an example can serve a model where metalic conducting islands (e.g. ordered crystalline phases), with mechanism described by eqn. (1.20) takes place, are separated by insulating barriers (e.g. amorphous phases) with the conduction through

FIT or VRH.

Furthermore, there are not only the stand alone CPs produced but they are often blended together with insulating materials in order to gain from the advantages of both types. In these cases conductivity is usually driven by percolation behaviour where a conductive path (an infinite cluster) is formed above the percolation threshold. The percolation ideas were also important in above described models, since hopping is often considered as a correlated bond-site percolation problem, or the critical path method was used e.g. in granular metal model derivation [17]. The typical dependence of the conductivity on the content (e.g. volume fraction) of a conductive phase ϕ above its critical value ϕ_C is [20]:

$$\sigma = \sigma_0(\phi - \phi_C)^p \tag{1.31}$$

where exponent p is 2 in the case of a 3D network of rigid spheres with conductivity σ_0 embedded in an insulating medium. But other models were also proposed such as the two-cut Gaussian with $p = 1.2$ where only a thin interfacial film separates the bulk phases giving a very low percolation threshold [21]. An overview of other models, 2D and 3D random resistors networks, with p from 1 to 2 can be found in ref. [22]. Besides the continuous 'geometrical' network percolation models also works counting with a tunnelling mechanism were published and these models provide a rather 'electrical' conductive network [23].

1.2.3 Transport mechanisms in AC conductivity

As noted before, a description of the system response on the frequency dependent electric field can be equivalently done in terms of complex dielectric function or complex conductivity. A lot of models for the AC conduction were developed from the relaxation time framework (described in the following section), and thus making differences between the 'dielectric' and the 'conductivity' approach is rather artificial. It may be considered as a matter of various points of view or an emphasis of the different aspects. Certainly, there are scientists who condsider the electrical conductivity as a more fundamental and a more general property then dielectric function and they even propose the same origin of the DC and the AC conductivity [24].

Similarly as in DC conductivity, for CPs the majority of models was 'borrowed' from the disorder semiconductors physics [25, 26]. The reason is simple: the AC conductivity shows some kind of 'universality', A very similar behaviour for different systems such as ion conducting glasses, amorphous/semicrystalline semiconductors, transition metal oxides, electron/ion conducting polymers, etc. [27]. Hence, there is 'universal' power law, proposed by Joncher, which together with DC conductivity is usually used in the form [28]:

$$\sigma'(\omega) = \sigma_{DC}\left[1 + \left(\frac{\omega}{\omega_c}\right)^s\right] \tag{1.32}$$

with exponent s lower than 1 and the characteristic plateau for frequencies lower than critical one ω_c. This critical frequency, moreover, is proportional to σ_{DC} known as the Barton-Nakajima-Namikawa relation. An increase in the conductivity can be understood even on macroscopic level (the disorder is on a macroscopic level) within the effective medium approximation, when the system is composed from different phases with different conductivities and while at low frequencies the overall conductivity is limited by the less conductive phases (in terms of a percolation path), in the high frequency regime the movement on a low scale is enhanced [29].

The exponent s can be derived from the microscopic models, and it is often frequency dependent, too. There could be two different mechanisms recognized, either the quantum mechanical tunnelling through a barrier (e.g. electron, polaron tunneling) or the thermally activated 'hopping' over a barrier (e.g. correlated barrier hopping) [25, 26]. Some of them are presented below. When the transport is driven by the electron tunneling, i.e. variable range hopping, then the real[2] part of the conductivity is expressed by:

$$\sigma'(\omega) = \frac{Ce^2 k_B T}{\alpha} N^2(E_F)\omega ln^4(\omega_{ph}/\omega) \tag{1.33}$$

with the numeric constant C which differs from author to author. And consequently s:

$$s = 1 - \frac{4}{ln(\omega_{ph}/\omega)} \tag{1.34}$$

with ω_{ph} phonon frequency $\sim 10^{13}\ s^{-1}$. When electon movement is followed by lattice relaxation and a polaron is formed, subsequently the energy is lowered and in the case of small (molecular) polarons, the conductivity is given by the same relation as before but with the exponent s:

$$s = 1 - \frac{4}{ln(1/\omega\tau_0) - W_H/k_B T} \tag{1.35}$$

with W_H the activation energy for polarons and τ_0 the characteristic relaxation time again of order of optical phonons. When polarons are big enough and the polaron clouds of distortion of the lattice overlap, the conductivity reads:

$$\sigma'(\omega) = \frac{\pi^4}{12} e^2 (k_B T)^2 N^2(E_F)\omega \frac{\omega R_\omega^4}{2\alpha k_B T + W_{H0} r_0 / R_\omega^2} \tag{1.36}$$

with R_ω the characteristic tunnelling distance. The coefficient s is now temperature and frequency dependent:

$$s = 1 - \frac{1}{R'_\omega} \frac{4 + 6W_{H0} r'_0 / k_B T R'^2_\omega}{(1 + W_{H0} r'_0 / k_B T R'^2_\omega)^2} \tag{1.37}$$

[2]In this section we usually omitt the expressions for the imaginary part of the conductivity due to its little interest in the work.

From thermally activated mechanisms we mention the correlated hopping of electrons when the Coulomb wells of two sites overlap and the conductivity is given by:

$$\sigma'(\omega) = \frac{1}{12}\pi^3 N^2(E_F)\epsilon\epsilon_0\omega R_\omega^6 \tag{1.38}$$

and s:

$$s = 1 - \frac{6k_BT}{W - k_BTln(1/\omega\tau_0)} \tag{1.39}$$

Another hopping-based model for the frequency dependent conductivity was proposed by Dyre [24] as the random free-energy barrier model where the hopping of charge carriers occurs in the presence of randomly varying energy barriers, evaluated by the continuous random walk and the effective medium approximation, giving the complex conductivity:

$$\sigma^*(\omega) = \sigma_0 \frac{i\omega\tau}{ln(1 + i\omega\tau)} \tag{1.40}$$

and exponent s:

$$s = 1 - \frac{2}{ln(\omega\tau)} \tag{1.41}$$

Apart from the fact that this model is based on several simplifications, it emphasises mainly that DC and AC conductivity are rather of the same origin. Furthermore, it was successfully used for the explanation of different experimental data [29].

For the heterogeneous system, which consists of the spherical conducting islands (indexed 1) with the volume fraction η separated by an insulating matrix (indexed 2) (e.g. PANI) Bianchi [30] used the random free-energy barrier model and within the effective medium approximation derived a relation for the total complex conductivity as:

$$\sigma^*(\omega) = i\omega\left[\epsilon_{2d} - \frac{i\sigma_2^*(\omega)}{\epsilon_0\omega}\right] \frac{2(1-\eta)\left(\epsilon_{2d} - \frac{i\sigma_2^*(\omega)}{\epsilon_0\omega}\right) - (1+2\eta)\frac{i\sigma_1}{\epsilon_0\omega}}{(2+\eta)\left(\epsilon_{2d} - \frac{i\sigma_2^*(\omega)}{\epsilon_0\omega}\right) - (1-\eta)\frac{i\sigma_1}{\epsilon_0\omega}} \tag{1.42}$$

1.2.4 Dielectric spectroscopy of polymers

Apart from the charge transport phenomenon there is also the dielectric response of a material coming from the microscopic fluctuations of molecular dipoles. We have already mentioned that it can be expressed by the complex permittivity $\epsilon^*(\omega)$. For the polymers as traditionally insulating materials, several metods of evaluation were developed or adopted [31]. The very basic model that links together the macroscopic polarisation and the microstructure of dielectric material was suggested by Debye. It is based on a single relaxation time τ that the system needs to reestablish its equilibrium state after the interaction with the external electromagnetic field. Within this approach the movement of an electric dipole in a double well potential distorted by an applied external electric field can be discribed. Or the movement of an isolated

fluctuating dipole in viscous medium in the presence of a stochastic force is described as well [4]. It results in the simple exponential decay of the polarisation in time and within the frequency domain $\epsilon^*(\omega)$ is expressed:

$$\epsilon^*(\omega) - \epsilon_\infty = \frac{\epsilon_s - \epsilon_\infty}{1 - i\omega\tau} \tag{1.43}$$

giving the symetric peak in $log\,\epsilon''$ vs. $log\,\omega$ with its maximum at a frequency proportional to the reciprocal value of the relaxation time $\omega_m \sim 1/\tau$. During an evaluation one should not forget also σ_{DC} contribution to ϵ'' given by eqn. (1.6). However, there can be more than one relaxation times which follow the distribution function $g(\tau)$ and the expression for $\epsilon^*(\omega)$ is modified:

$$\epsilon^*(\omega) - \epsilon_\infty = (\epsilon_s - \epsilon_\infty) \int_0^\infty \frac{g(\tau)}{1 - i\omega\tau} d\tau \tag{1.44}$$

Based on this distrubion function of the relaxation times several phenomenological models were suggested to describe experimental data with τ as the relaxion time with the highest probability, i.e. Cole-Cole function with also symetrical peak of ϵ'':

$$\epsilon^*(\omega) - \epsilon_\infty = \frac{\epsilon_s - \epsilon_\infty}{1 - (i\omega\tau)^\alpha} \tag{1.45}$$

and the exponent α varying from 0 to 1 when it reduces itself into the Debye model thus expressing width of the distribution. Other proposed models, for the rather asymmetric loss peaks, are the Cole-Davidson function:

$$\epsilon^*(\omega) - \epsilon_\infty = \frac{\epsilon_s - \epsilon_\infty}{(1 - i\omega\tau)^\beta} \tag{1.46}$$

and the most generallised Havriliak-Negami function:

$$\epsilon^*(\omega) - \epsilon_\infty = \frac{\epsilon_s - \epsilon_\infty}{(1 - (i\omega\tau)^\alpha)^\beta} \tag{1.47}$$

with the parameters α and β related to the shape of loss peak.

It was observed that the position of a loss peak maximum is shifted to the higher values with increasing temperature. Consequently, some expressions for the temperature dependencies were proposed such as the exponential Arrhenius function:

$$\omega_m(T) = \omega_\infty exp\left(-\frac{E_a}{k_B T}\right) \tag{1.48}$$

with the activation energy E_a of the relaxation process often successfully used for polymers in a glass state describing the so called β-relaxation. This usually arises for amorphous polymers from the localized rotational fluctuation of dipoles. Another temperature dependence has a form of the Williams-Landel-Ferry equation:

$$log\frac{\omega_m(T)}{\omega_m(T_{ref})} = -\frac{c_1(T - T_{ref})}{c_2 + T - T_{ref}} \tag{1.49}$$

with T_{ref} as the reference temperature and c_1, c_2 the so called WLF-parameters. This behaviour is typical for the α-relaxation (the glass transition) when the polymer chains become more mobile promoting the dielectric spectroscopy to a powerfull tool for the glass transition investigation. In the literature also the Vogel-Fulcher-Tammann equation can be found for this case but it is mathematically equivalent to eqn. (1.49) [32].

There is also another mechanism which contributes to the dielectric response, but unfortunately it often complicates the evaluation. It is the separation of charges at interfaces. At the mesoscopic level for the inhomogeneous mixtures it is also known as the Maxwell-Wagner-Sillars polarisation and in a low frequency regime there is a typical strong contribution to ϵ' and a change in slope for ϵ'' in $log\,\epsilon''$ vs. $log\,\omega$ plot. Even more significant, the several orders of magnitude in ϵ' higher than the proper dielectric response, can be a contribution from the electrode polarisation common for conductive samples where the charge carriers are blocked at sample-electrode interface. Its frequency spectrum can be described by the fractal laws [31].

1.2.5 Applications

Even if the discovery of conductive polymers has brought a lot of excitement among researchers, their possible applications are still at the begining and their usage is far away from the conventional (semi)conductors. It is true that CPs as the polymeric materials are low weighted and with their high tensile strenght. Moreover provide the electrical conducitivity within a wide range to compete with the conventional materials, but it seems to be improbable that CP would cause some kind of a technological revolution or replace wide spread materials of today. But they can be implemented in those kinds of industry where their advantages make them superior to the traditional materials.

There are several applications where CP can be successfully used: electromagnetic shielding, field smoothening in cables, capacitors, through-hole electroplating in printed circuit industry, antistatic devices, polymer batteries, electrochromic displays, electrochemical sensors, solar cells, FET, O-LED, etc. [3]:

1.3 Polyaniline

Polyaniline is the oldest prepared conducting polymer and has been known to the mankind since the nineteeth century. A deeper interest as is nowadays started after a discovery of conducting polymers in 1970s. Since then a huge effort has been made to investigate its properties and a lot of progress has been made. A summarized

basic knowledge about PANI can be found for instance in ref. [33, 34]. PANI is especially interesting due to its cheap and straightforward preparation, its thermal and environmental stability and simple non-redox doping. It can be syntetized in five various oxidation states from fully oxidized leucoemeraldine, through protoemeraldine, emeraldine and nigraniline, to fully reduced pernigraniline. The typical preparation route (fig. 1.2) is the oxidation of aniline in ammonium peroxodisulfate and the aqeous acid environment (with pH 0-1). The product of this reaction is already a polyaniline salt which is partly crystalline and has 9-10 orders of magnitude higher electrical conductivity than emeraldine base. For instance, HCl (with the molar concentration 1 mol/l) doped PANI has its room temperature conductivity about 1-5 S/cm when compressed into a pellet [34]. This doping process, so-called protonation by acids, is unique and the total number of electrons is conserved in contrast to redox doping common for the rest of CPs.

Except the acetic acid, plenty of others protonic or pseudo-protonic aqueous acid can be used to prepare PANI salts what influence overall conducitivy of the system as well as the morphology, e.g. nanotubes or granular morpohology [35]. Apart from the elecrical conductivity enhancement, doping with camphor sulphonic acids improve its solubility because PANI in undoped state tends to aggregate due to the strong hydrogen bonds and thus is insoluble in common solvents [33]. Furthermore, PANI can be synthetised in the form of oriented films or oriented fibres what results in a significant increase in a preferred direction (up to 80 S/cm) [34].

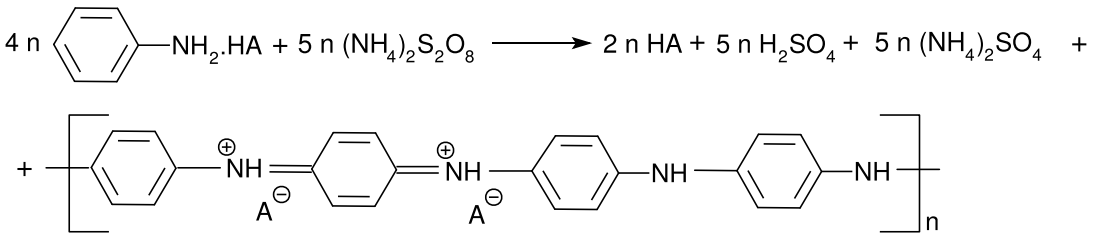

Figure 1.2: Preparation of emeraldine salt according to ref. [36], i.e. HA is HCl.

Because PANI contains benzene rings (both bezoid and chinoid) there are the non-degenerated energy ground states and after doping polaron and bipolaron quasiparticles are crated. Also a free electron pair on the nitrogen atom contributes to a conjugational system. On the basis of several measurements (the magnetic properties, the X-ray diffraction, the conductivity and the thermopower, etc.) the granular metal model was proposed for PANI where the formation of completely doped ('metallic') islands in an insulating matrix takes place and the charging energy limits the tunnelling process [34].

Chapter 2

Experimental techniques for AC/DC σ measurements

2.1 Methods for DC conductivity measurements

As we have already seen, the electrical conductivity, respectively the resistivity is an important parameter not only from the technological point of view in possible applications but from scientific as well. There is a hidden information about the physical transport phenomenon. It is then important to be able to measure the conductivity experimentally with a satisfactory precision. In fact, a measurement of the conductivity is practically reduced to a measurement of the electrical resistance (or better the voltage U and the current I) and its recalculation in respect of the dimensions of a sample. There are several techniques to achieve it, each with its strength and weakness, and some of them are described below.

There are several methods referred as contact using methods, such as the two-point probe, the four-point probe, the differential Hall effect, the spreading resistance, the applied current tomography [37]. The first two of those above mentioned methods were used in our work and therefore they are going to be described in more details.

The two-point probe method (fig. 2.1a) surely belongs to the easiest ones at least from the implementation point of view. There is a need only for two probes where each acts as a voltage and a current probe. But the problem arises when one would interpret the measured data. Because what in fact is measured is the total resistance R_T:

$$R_T = \frac{U}{I} = 2R_p + 2R_c + 2R_{sp} + R_s \tag{2.1}$$

which consist of the probe resistance R_p, the contact resistance R_c at probe-sample contact, the spreading resistance R_{sp} when current flows from a small metal probe into the sample and *vice versa* and, finally, the sample resistance R_s. One can notice

that in this method one has to deal with three parasitic resistances where only the probe resistance can be determined separately by measuring at shorted probes. The rest of them can not be determined and one has to be aware of it while interpreting the results.

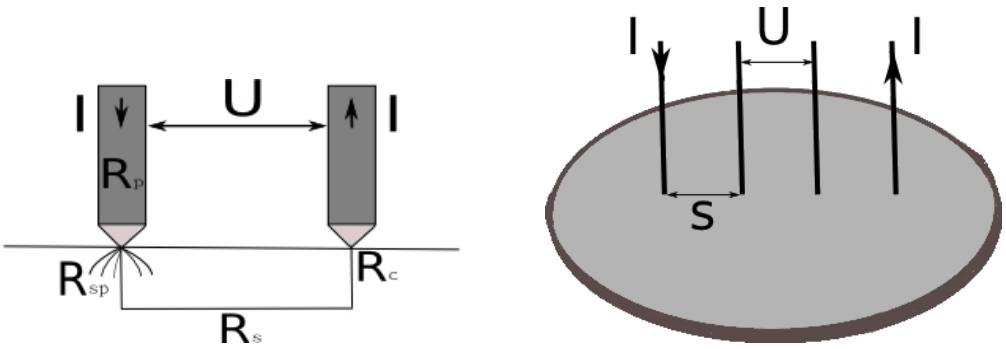

(a) (b)

Figure 2.1: The two-probe method with the parasitic resistances (a) and the four-probe method with an equidistant alignment of the probes s (b).

One way how to get rid of the parasitic resistances is to use the four-point probe method (fig. 2.1b) where two probes serve as current probes and two as voltage probes. The voltage probes are free of the parasitic resistances (that are negligible) due to small currents while the voltage is being measured. When the spacing s between the probes is equidistant and the finite dimensions of a sample are taken into account, the resistivity can be written in the form:

$$\rho = \frac{1}{\sigma} = 2\pi s \frac{U}{I} F \tag{2.2}$$

with F as a correction factor concerning the sample geometry, the thickness, the probe displacement and the distance from edges. But this configuration is still dependent of the geometry of the sample what sometimes could cause problems. However, Van der Pauw [38] showed that an arbitrary shape sample (fig. 2.2a) can be used and the resistivity can be determined easily when the sufficiently small contacts are placed at circumference of the uniformly thick singly connected sample. These ideas are based on some relations derived from the basic electrodynamics and generalized to arbitrary shape samples by conformal mapping. One can obtain the expression for the resistivity which is even more simplified for symmetrical samples (e.g. circle, square):

$$\rho = \frac{\pi t (R_{12,34} + R_{23,41})}{2ln(2)} F = \frac{\pi t R_{12,34}}{ln(2)} \tag{2.3}$$

with $R_{12,34}$ the resistance where the current enters a sample at contact 1 and leaves at 2 and the voltage is measured between the contacts 3 and 4. If in this arrangement the contacts are placed in the corner of an imaginary square, a relative error introduced by the finite displacement d from the circumference of a round sample with the

diameter D (fig 2.2b) could be determined as:

$$\frac{\Delta\rho}{\rho} = -\frac{d^2}{2D^2 ln(2)} \tag{2.4}$$

Except this error there are other factors that can introduce errors into the measured values such as the electric current itself due to heating of a sample and the minority/majority carriers injection. This is more important for more conductive samples as higher currents are essential to obtain measurable voltages. Another error is caused by the temperature due to the possible thermoelectric voltage. For more resistive samples a surface leakage currents can cause errors and a guard ring held at a similar potential as a probe should be used [37]. Even if at first sight it could seem that resistivity measurements are easy to perform, one should be aware of many different factors to obtain reasonable and as error-free values as possible in order to deal with the real properties of materials.

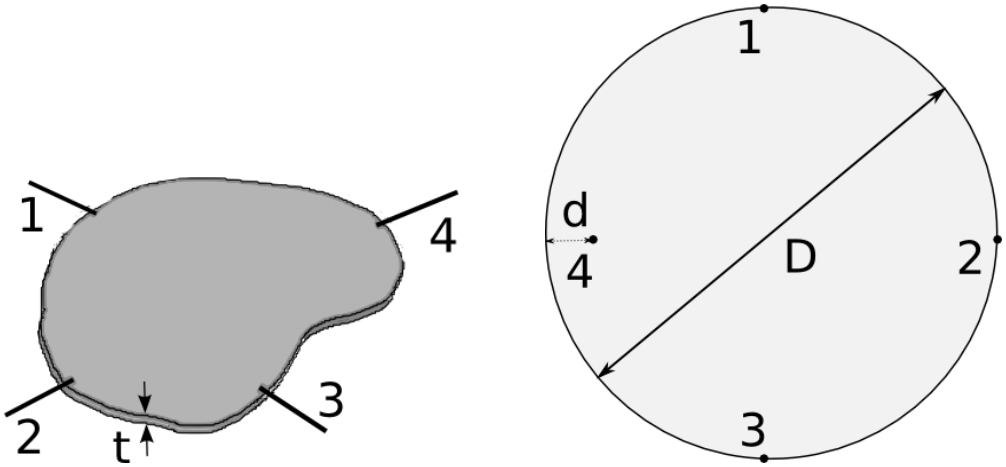

Figure 2.2: The Van der Pauw configuration for an arbitrary shape sample (a) and the displacement of the contact from a circumference (b).

There are also other techniques available. For instance the differential Hall effect or the spreading resistance measurements are useful when one is interested in the depth profile of the sheet resistivity in non-uniformly doped semiconductors. When contacts are unwilling (e.g. for the non-destructive measurements) there are also the so called contact-less methods based on the eddy currents or using the confocal resonator [37]. But these methods provide AC conductivity which is not necessarily the same as DC conductivity. Nevertheless, the more detailed description of these methods lies beyond the scope of this work.

2.2 Methods for AC conductivity measurements

In general, the complex dielectric function or conductivity (eqn. (1.7)) can be measured in a very wide range of frequencies, $10^{-6} - 10^{12}$ Hz, and several different approaches [39] have to be used to cover the whole interval. The lumped circuit methods, where a sample represents the parallel or the serial circuit of an ideal capacitor and an ohmic resistor, can be used in frequency range from $10^{-6} - 10^{7}$ Hz limited at high frequencies by the geometrical dimensions of the capacitor and parasitic impedances caused by cables. As this frequency range is the object of our study, we will describe the (used) methods in more details below. For higher frequencies, $10^{7} - 10^{11}$ Hz, there are methods used, which are based on the measurement of the complex propagation factor are used. For even higher frequencies the quasi-optical devices such as different interferometers are employed. Another approach, at frequencies $10^{-6} - 10^{10}$ Hz, can be a measurement of the time dependent dielectric function followed by the Fourier transformation given by eqn. (1.9).

When a sample is put into a capacitor (with vacuum capacitance C_0), its $\epsilon^*(\omega)$ can be defined by its complex capacity, but in principle, within a linear response is reduced to a measurement of the complex impedance $Z^*(\omega)$ (or better the current and the voltage):

$$\epsilon^*(\omega) = \frac{C^*(\omega)}{C_0} = \frac{1}{i\omega Z^*(\omega) C_0} \tag{2.5}$$

There are two principally different techniques to obtain the complex impedance and both were used in this work: the dielectric converters with the Fourier correlation analysis often implemented in integrated dielectric analysers (e.g. α-analyser from Novocontrol) and the impedance analysis implemented in AC impedance bridges (e.g. HP precision LCR meter).

The former one is based on two vector voltage analysers (converters) that analyse a time response of a sample on the applied time dependent voltage. In order to work within a wide range of the impedances, the dielectric converters that use the broadband electrometer amplifier with a variable gain are preferred. An example of the final circuit scheme with the internal reference capacitor of the impedance Z_R^* is at fig. 2.3 with the measured sample impedance:

$$Z_S^*(\omega) = \frac{U_{1S}^*(\omega)}{U_{2S}^*(\omega)} \frac{U_{2R}^*(\omega)}{U_{1R}^*(\omega)} Z_R^*(\omega) \tag{2.6}$$

This approach with the reference capacitor is mainly useful at high impedances, otherwise the accuracy of the measurement is reduced.

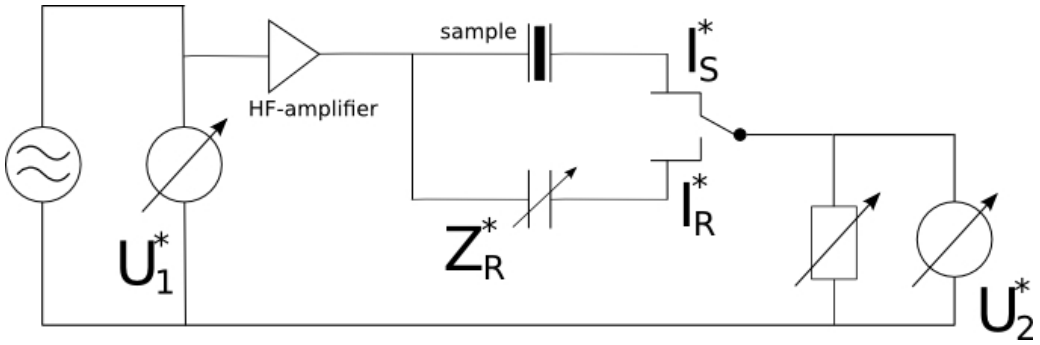

Figure 2.3: An example of electrical circuit for the dielectric analyser according to ref [39].

The later, with a scheme on fig. 2.4, which is used on balance of currents I_S^* flowing through a sample caused by the known voltage from the generator and I_C^* flowing through the compensation impedance. When the bridge is balanced, the impedance $Z_S^*(\omega)$ is given by:

$$Z_S^*(\omega) = -\frac{U_S^*(\omega)}{U_C^*(\omega)} Z_C^*(\omega) \tag{2.7}$$

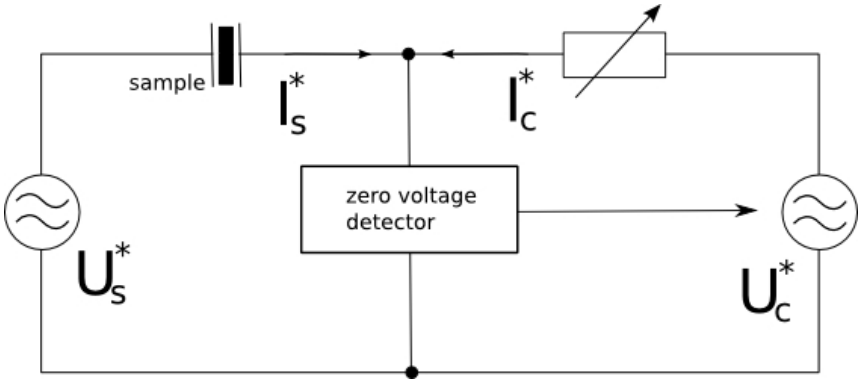

Figure 2.4: An example of electrical circuit for the impedance bridge according to ref [39].

Chapter 3

Experimental

This chapter briefly describes the experimental setup used in our work. The AC and DC characteristics of studied materials were obtained by using of several different methods which were theoretically described in previous chapter. Each of them was automatized by computers with (either commercial or self-written[1]) specific controlling programs.

The DC conductivity measurements concern:

- Four-point probe method in the Van der Pauw (VdP) configuration - formed of a sample holder with four platinum-rhodium alloy pin contacts, Keithley 237 Voltage Source and Keithley 2010 multimeter. Lake Shore 332 Temperature Controller and Janis VNF-100 Cryostat were used for temperature dependencies. The pressure during this experiment was sensed by Pfeiffer Vacuum Dual Gauge.
- The two-probe method - consisted of a shielded sample holder and Keithley 6517 Electrometer.

All samples whose temperature dependences were studied and the VdP technique was used, were followed by a procedure where at first they were treated for about 2×10^4 s at ca 305 K in vacuum. This was established after approximately 1500 seconds and the low pressure in a chamber (where the samples were held) of ca 10 Pa (achieved by the rotary air pump). This remained more or less the same during the whole experiment, as did the temperature (fig 3.1) and the time characteristics were obtained. This part of the procedure also served as preparation for measurements as was expected that the samples would lose their moisture level. Later the temperature characteristics at cooling as well as heating rate were obtained within the range 77-315 K where the liquid nitrogen was used as the cooling medium. The

[1] a sincere acknowledgement belongs to Dr. Ivo Křivka who is an author of the majority of programs

values of measuring currents were tuned in respect to the resistivity of the samples in order to avoid high Joule heating, as well as to achieve a measurable voltage. A relative standard deviation usually better than 1% was achieved. This deviation, however, does not account for any contact displacement error, or any possible small variation in the resistivity with measuring current.

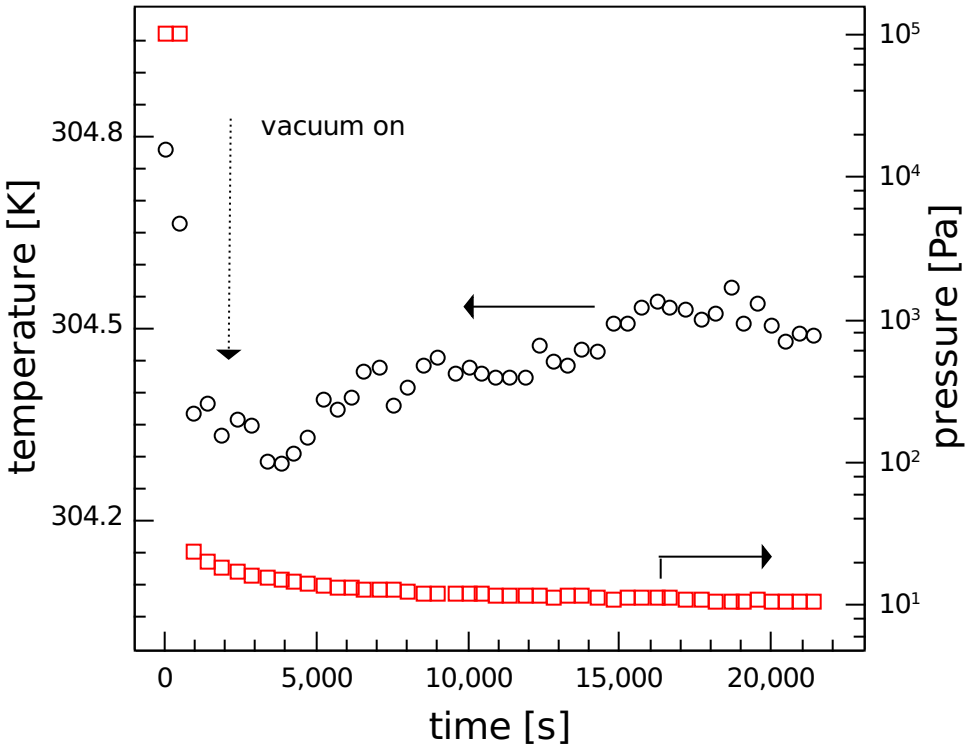

Figure 3.1: The temperature and the pressure profile during the VdP experiment.

For the AC conductivity measurements three following techniques were used:

- AC modification of DC VdP method - it consisted from a sample holder with four pin contacts, which were connected to Keithley 6221 DC and AC Current Source, Keithley 7002 Switch System and Keithley 2010 Multimeter
- auto balancing bridge method - performed by Hewlett Packard 4284A LCR meter in the four-terminal pair configuration within the frequency range of 20 Hz-1 MHz [40]
- I-V method based on dielectric converter and Fourier correlation analysis - consisted of a sample capacitor cell shielded by cryostat, Novocontrol α-analyser with frequency range $10^{-1} - 10^6$ Hz and embedded temperature controller that enabled as high precision of temperature as 0.1 °C [41]. The temperature range from -160 to 30 °C was provided by flow of nitrogen vapours.

In all above mentioned measurements, the applied AC voltage was chosen in respect of the resistivity of samples. It should be noted that all samples were in the form of pellets with a diameter 13 mm and for all measurements, except VdP, golden electrodes had to be evaporated on, either with diameter 10 mm or 8 mm and a guard ring at circumference.

Images of pellets surface were taken by Dino-Lite digital microscope at a magnitude of 30-60 times.

Chapter 4

Results and discussions

In this chapter our attention is focused on the experimental results and their interpretation. It is divided into two mostly independent sections where two different systems based on polyaniline were studied: polyaniline-silver (PANI-Ag) nanocomposites and polyaniline-montmorillonite (PANI/MMT) composites.

4.1 Polyaniline-silver nanocomposites

4.1.1 Introduction

This section is dedicated to the nanocomposites of PANI containing silver nanoparticles. The aim of our work was to investigate the electrical properties (DC conductivity) of a material with the presence of a classically very good conductor - silver and semiconducting PANI in one composite. Moreover this kind of materials are very interesting from the chemical point of view, as our samples were prepared[1] by polymerisation of aniline where reduction of silver nitride takes place (see fig. 4.1). It means that from originally two non-conducting components (aniline and silver nitride) the conducting composite is achieved consisted from two conducting components [42].

As we already know, to reach a reasonable value of the electrical conductivity, PANI has to be doped, for instance converted to a salt by the protonation with an acid, otherwise PANI would be in the base state, which is insulating. All samples were protonated by nitride acid which is an inevitable byproduct of the polymerisation process (fig. 4.1) but also others acids were used as dopants [42]. Our study is based on protonation of PANI by various sulfonic acids as methanesulphonic (MSA), toluenesulfonic (TSA), aminosulfonic (SFA), camphorsulfonic (CSA) and acetic acid (AC),

[1] the Institute of Macromolecular Chemistry of Academy of Sciences of the Czech Republic, Prague

formic acid (FA) as well. These acids were in the aqueous solutions at different concentrations.

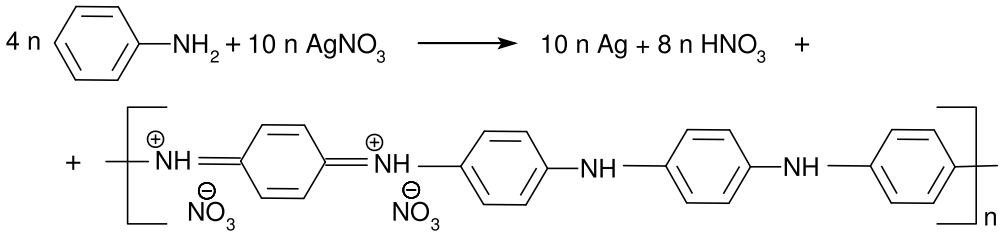

Figure 4.1: The preparation of PANI/Ag composites according to ref. [42].

For a better understanding of the electrical transport, it is crucial to have some information about the morphology and the composition of materials. First of all, these composites are not only a mixture of two independent parts which were blended together. As we mentioned above, they come from the polymerisation process and form the nanostructures as it was shown by TEM [42, 43]. In the case of the sulfonic acids (CSA, TSA, MSA), there are silver nanoaggregates of a size about 50 nm with occasional tendency to form clusters on PANI hairy nanorods and the structure is more or less similar for all samples. One can even observe some differences in distribution of silver particles [42]. For acetic acids except the spherical silver nanoagregates of a diameter of ca 25-50 nm also silver nanorods with a diameter ca 300 nm can be found. But since there is no information about the percentage of the different types of morphology in samples, it can not be simply concluded which morphology 'belongs' to which sample [43]. The presence of protonated PANI was confirmed by FTIR and Raman spectroscopy and the content of silver in the composites was measured by TGA and values 63-72 w.t.% (close to the theoretical ones, 68.9 %) were found out [42, 43]. But rather than the exact value, important is that all samples contain more or less the same amount[2] of metallic silver (with one exception - SFA, see table 4.1).

In this scope of the work we are studying the DC conductivity at a room temperature and the effect of ageing, the temperature dependences and the time dependences at the constant temperature and pressure in respect of various dopants and their concentration by using the experimental methods and devices described in chapters 2 and 3, in concrete VdP method. The theoretical models were also fitted to the experimental data and the transport mechanisms were suggested.

Most of the results presented here in the temperature dependences of the conductivity were obtained at different currents and in a heating mode. The results at cooling

[2]vol % of silver in composites were calculated from TGA w.t.% data according to ref. [42, 43] and density of silver [44]

are not presented due to the difficult temperature control at a lower part of the temperature interval but generally they agreed well with heating mode data. The data which were obtained at the biggest current are presented where it was possible. But the results were usually current independent (an ohmic behaviour) with only few exceptions. Then only ohmic ones were taken as the 'valid' results. The last, but not the least issue was the technological one, where sometimes two samples prepared in the same way and at the same initial conditions gave different results what calls for either better preparation controlling or better statistics.

4.1.2 Temperature dependences

The temperature dependences of the conductivity, generally, provide interesting information because they are related to the transport mechanism as we mentioned in chapter 1. The results are shown in the figure 4.2. For the dopants TSA, SFA, CSA, FA, we can see an increase in the conductivity which is typical for organic semiconductors such as PANI salt (see CSA-without Ag for a comparison, fig. 4.3); however, for AC and MSA, the conductivity shows metallic behaviour, even though the bulk silver conductivity is much higher, ca 10^5 S/cm, and above 100 K its resistivity increases linearly with the temperature [45, 46]. Regarding our samples the conductivity is much lower, about $10^2 - 10^3$ S/cm, and the linear increase in the resistivity is full filled only for some samples respectively for all samples but only at higher temperatures.

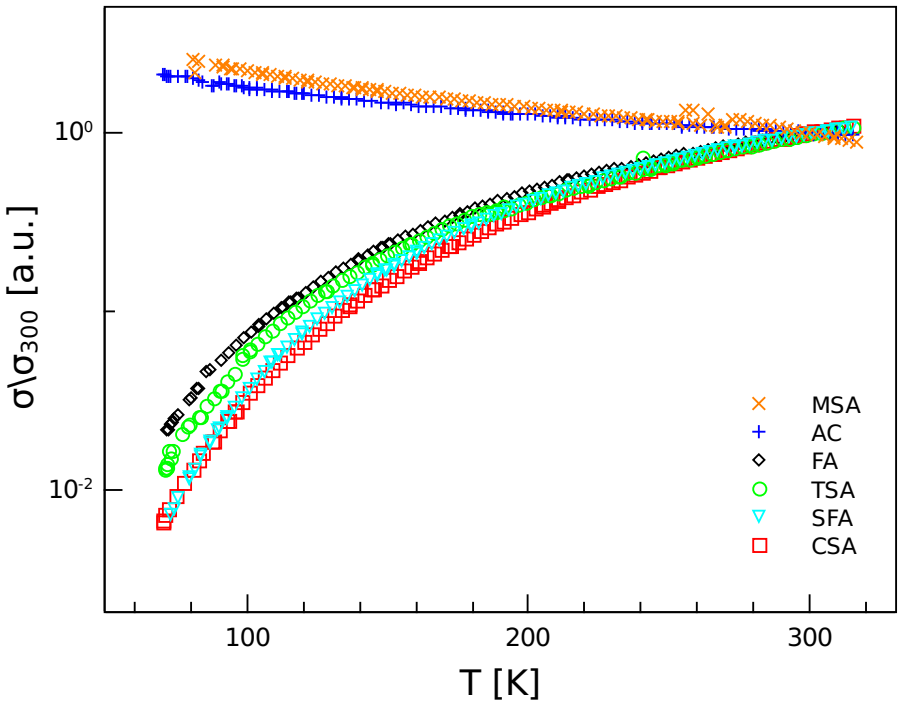

Figure 4.2: The temperature dependence of PANI-Ag conductivity for different acids.

There are summarized values of conductivity (at 300K, extracted from σ vs. T plot, what we believe are values more related to material due to its moisture evacuation) and the temperature behaviour for all samples in table 4.1. It should be noted that these values are still serving rather for the orientation, since they slightly vary with ageing or for samples repeated, the powder was recompressed, (e.g. CSA:075) and sometimes they change intensively with sample's reproduction and can also vary within one order of magnitude (e.g. CSA:0.5). Nevertheless, it is obvious that for some dopants (AC, MSA, FA, SFA) the conductivity of the composites is 10 - 1000 times higher than common few S/cm typical for the protonated PANI pellets [34].

sample	$M_{acid}[mol.l^{-1}]$	$t\,[cm]$	$\phi_{Ag}[vol.\%]$	$\sigma_{300}[S/cm]$	S/M
PANI/AC-Ag	1	0.069	24	3600	M
PANI/MSA-Ag	1	0.099	25	1300	M
PANI/FA-Ag	1	0.042	–	48	S
PANI/TSA-Ag	1	0.075	22	0.8	S
PANI/CSA-Ag	1	0.088	19	1.5	S
PANI/SFA-Ag	1	0.087	3	25	S
PANI/AC-Ag	1	0.069	24	3600	M
PANI/AC-Ag	5	0.066	23	2300	M
PANI/AC-Ag	0.5	0.055	22	310	M
PANI/AC-Ag	0.2	0.060	24	260	M
PANI/CSA-Ag	0.75	0.085	–	0.054	S
PANI/CSA-Ag	0.5	0.072	–	7.4	S
PANI/CSA	1	–	–	0.9	S
PANI/CSA-Ag	0.75	0.085	–	0.054	S
PANI/CSA-Ag(R)	0.75	0.089	–	0.067	S
PANI/CSA-Ag	1	0.088	19	1.5	S
PANI/CSA-Ag(R)	1	0.085	–	1.1	S
PANI/CSA-Ag	0.5	0.072	–	7.4	S
PANI/CSA-Ag(N)	0.5	0.084	–	0.79	S

Table 4.1: The volume content of silver, the conductivity at a room temperature and the temperature behaviour (S: semiconducting, M: metalic) for different dopants of PANI-Ag composites.

It is believed, that there is a strong contribution of silver to the overall conductivity, and even the temperature dependence behaviour could vary significantly. The composites show either the semiconducting behaviour typical for the PANI salt pellets on a insulating side of the metal-insulator transition or the metallic behaviour (fig. 4.2). We should keep in mind that the content of silver is in the most cases the same. That is why only amount of silver alone can not explain the experimental data. Moreover, conductivity differs in orders of magnitude.

If we compare our results with the conductivity of PANI-bases and silver composites which are about one order of magnitude lower in the case of acetic acid and several orders of magnitude in the case of sulphonic acids [42, 43], it is obvious that PANI somehow should assist in the charge transport. For example in the case of the low silver content and the low conductivities, the presence of conductive polymer seems to be crucial for the overall conductivity [47]. High weight content of silver in the polymer matrix-silver composites was achieved and reported in literature also for epoxy network-silver composites where the spherical silver nanoparticles of 50 nm were dispersed in insulating matrix and in the absence of the conductive path samples were insulated [48]. On the other hand, the metallic behaviour could be determined by the presence of silver nanorods. As it was noted above, this is supported by the high conductivity of blends with emeraldine bases when acetic acid was used as the dopant. For an explaination of the high values of the conductivity, a percolation-like hypothesis might be taken into consideration: in case of the absence, the low (volume) content or the non-uniform distribution of the metallic nanorods, one could expect a low conductivity with the semiconducting behaviour as a consequence of the absence of the metallic-like percolation path. On the opposite side, when the conductive path throughout the material is fully provided by these silver nanorods, the possible metallic conductivity with superior values similar to the bulk silver ones could be expected. If this was true, then our case would probably fall into the transition area between the semiconducting PANI-like and the metallic silver behaviour. Polyaniline matrix and silver nanoaggregates (especially while PANI bases were used) assist to achieve the conductive path through the hopping or other tunnelling processes. But within this hypothesis the metallic PANI/MSA-Ag[3] is hard to explain since any silver nanorods have not been observed.

An influence of the acid molar concentration on the temperature characteristics is presented on fig. 4.3 for CSA. We can see that in all cases we are dealing with similar semiconducting behaviour but the sharpness is changing. There is also a sample which does not contain any silver, included just for a comparison since it shows the typical behaviour of pure PANI/CSA samples. PANI/CSA:x(R) stands for another sample with M = x where a sample was repeated in terms of the powder recompression into pellet and as we can see, there is no significant difference. On the other hand PANI/CSA:0.5(N) behaves in a different way, and hence, overrides the effect of different concentration. Even if we suppose that the differences due to the molar concentration are the property of a material it is rather questionable in respect to the results for PANI/CSA:0.5. A more probable hypothesis seems to be that there are lots of factors during the technological processing affecting the electrical conductivity of a sample even if the conditions (temperature, pressure, acid, molar concentration, etc.) are almost the same. The table 4.1 and the figure 4.3 say that the relative changes are not directly related to the absolute values of

[3]further in the text the suffix -Ag is often omitted, especially when the molar concentration is discussed, because it is clear that in this section we have worked with the polyaniline-silver composites

the conductivity (because PANI/CSA:0.5(N) in that case should have behaved like PANI/CSA:1). For these reasons we have to conclude that a deeper analysis is not appropriate until the influence of the preparation process is revealed. Because the samples were not prepared at once, PANI/CSA-0.5(N) can not be just disqualified as the out of set prepared sample.

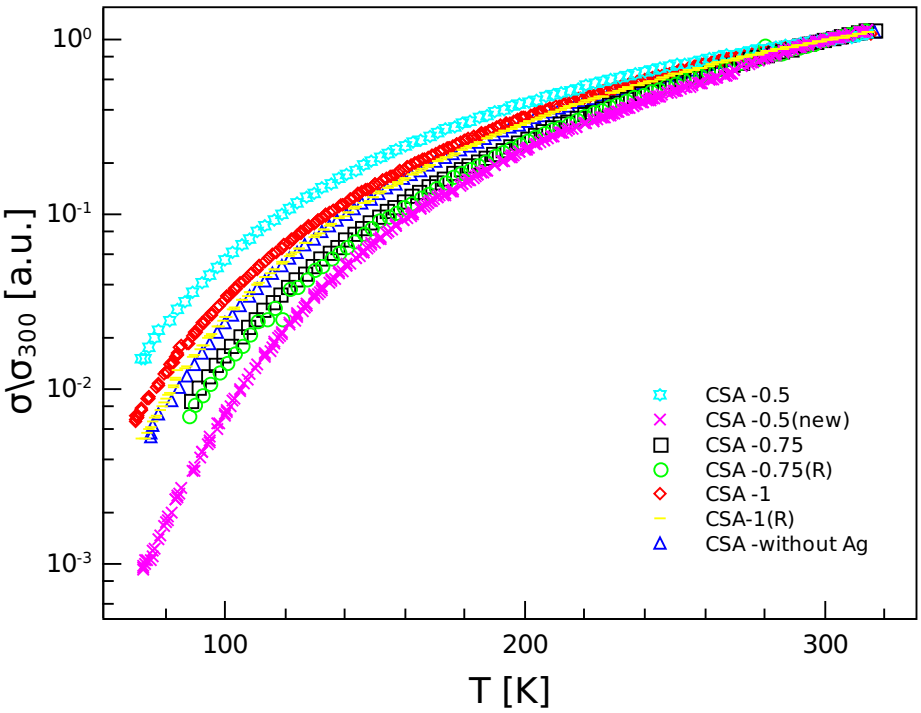

Figure 4.3: The temperature characteristics of the conductivity for the different molar concentration of CSA in PANI/CSA-Ag composites.

In the contrary to the results for semiconducting PANI/CSA-Ag samples, the temperature dependence of the metallic PANI/AC-Ag seems to depend on the molar concentration or better, on the absolute value of the conductivity (tab. 4.1 and fig. 4.4). It would be interesting to see whether samples with even lower conductivity could show the temperature independence or the transition to a semiconducting behaviour. If this was true, the metal-semiconductor transition and the tuning would be possible by chemistry variations. In order to achieve this we need to suppose that the absolute value of the conductivity is linked with the molar concentration of a dopant and we should reduce it, for instance, to 0.1 or 0.05 mol/l. Unforturnatelly, then we have to face the experimental issue, because at the such low concentrations of 'weak' acids (as acetic acid is) the polymerisation process will not occur [49].

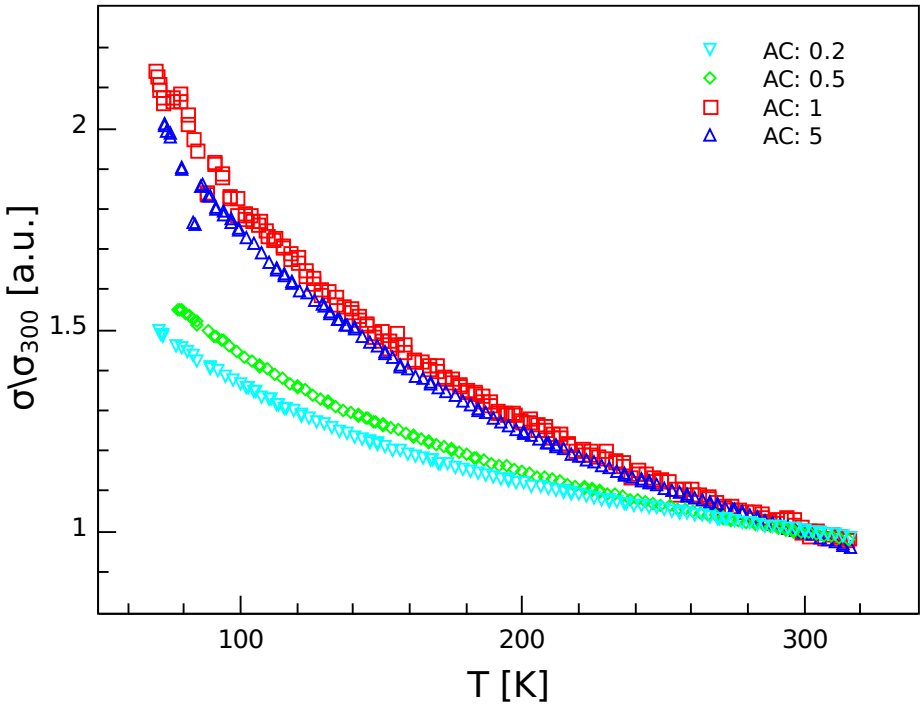

Figure 4.4: The temperature characteristics of the conductivity for the different molar concentration of AC in PANI/AC-Ag composites.

To shed at least little light on the charge transport mechanism we tried to fit[4] some known theoretical models where it was possible. The results are summarized in tables 4.2 and 4.3. The shape of the temperature dependences for PANI/CSA-Ag are similar to the reference sample and indicates that the often used theoretical model for pure CPs (e. g. VRH, FIT, CELT) might be used further on. For PANI/AC-Ag, PANI/MSA-Ag the typical metallic linear dependence of resistivity[5] can be applied. Other possibility based on the idea of heterogeneity, proposed by Kaiser [2], is a superposition of various known mechanisms weighted by the geometrical factors, eqn. (1.30), but we believe this approach is limited and appropriate only if there are no differences of orders of magnitude between different mechanisms (otherwise one of them can be neglected and a number of free parameters is reduced). There are a few examples of the fits, for PANI/AC:1 and PANI/CSA:0.5 on fig. 4.5-4.6.

The equation (1.16) was used for metallic samples, however, it was valid only for a shortened temperature range. It gave us a rather more technical parameter - the temperature coefficient of the electrical resistivity α_ρ. A commonly used value of this parameter for pure silver is 3.8×10^{-3} K^{-1} at a room temperature [50]. In our case, for the most conductive samples PANI/AC:1 and 5 two linear dependences in good agreement were obtained, the less conductive PANI/AC:0.2 and 0.5 only high

[4] used the Leverberg-Marquardt and the simplex method implemented in the program OriginPro
[5] it is more convenient for us to choose the resistivity approach instead of the conductivity

temperature linearity was observed. The experimental data for MSA samples were too 'disordered' at a high temperature so this range was omitted.

The obtained room temperature coefficients are lower than pure silver shows, what indicates that the increasing temperature (and thus the phonon scattering) has a smaller impact on the resistivity change. This would be probably caused by the reduced effect of silver in the composites since the coefficients are lower for the less conductive samples. For the high slopes (coefficients) at low temperatures, up to now, we do not have any explanation but a linear dependence is valid only to the temperatures about 150-200 K and then the slope is changed and described by a room temperature α_ρ. One more model for the metallic conductivity (eqn. 1.20) typical for anisotropic Q1D conductors was tested but without a success. As the metallic samples behaviour is similar to that for silver but the parameters are different, we conclude there should be, for this time an unspecified relationship or an interaction between the charge transports due to silver and PANI. From the metallic behaviour we at least conclude that the conductivity is mostly limited by the phonon scattering.

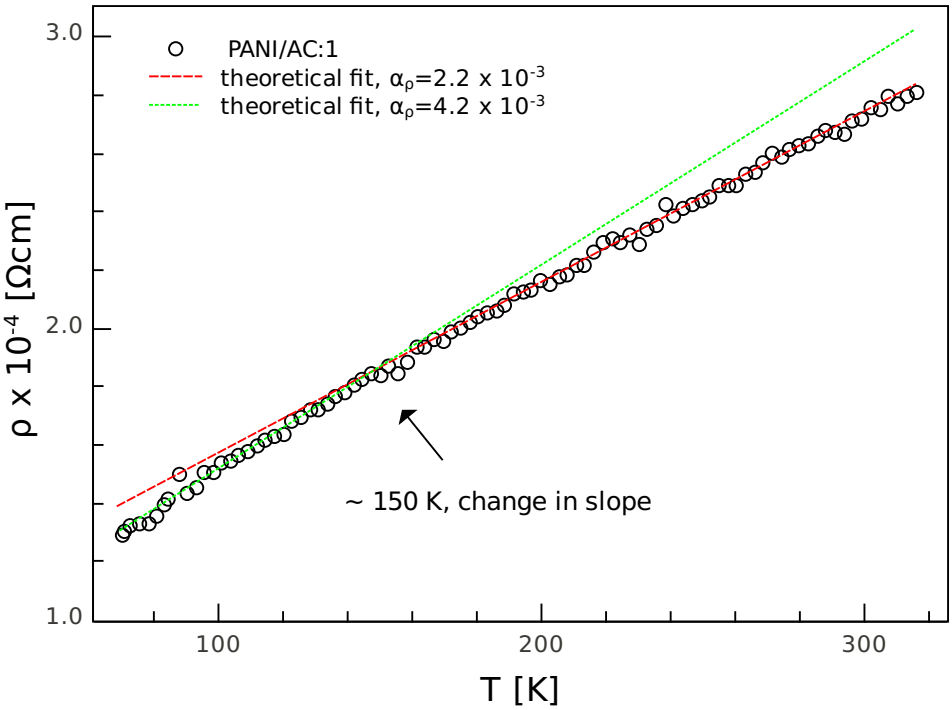

Figure 4.5: An example of the theoretical fit, PANI/AC:1.

sample	$T_r[K]$	$\alpha_\rho \times 10^{-3}\,[K^{-1}]$	$T_r[K]$	$\alpha_\rho \times 10^{-3}\,[K^{-1}]$
PANI/AC:0.2	300	1.0	–	–
PANI/AC:0.5	299	1.3	–	–
PANI/AC:1	299	2.2	96	4.2
PANI/AC:5	300	2.0	86	4.4
PANI/MSA:1	–	–	81	7.2

Table 4.2: The results of the fitting procedure for the metallic samples, T_r as the reference temperature.

In the case of semiconducting samples, we have noticed that while for the high temperatures data are well described by the activated 'Arrhenius' (ARH) $log\,\sigma \sim 1/T$ transport, for the lower temperatures, generally below 200 K, the conductivity mainly fits within $log\,\sigma \sim 1/T^{0.5}$ or the FIT. Other coefficients γ (e.g. 1/4, 1/3, 2/5) for the VRH models failed. Moreover, the FIT model did not have to be in a superposition with the ARH model to fit the whole temperature range. At times, the superposition gave even worse agreement with unreliable fit parameters. We conclude that ithe FIT model achieved a superior agreement with experiment for all semiconducting samples, in particular for those with the higher conductivities, $\sigma_{RT} \sim 10^0 - 10^1$ S/cm. The superposition of the VRH-like and the Arrhenius-like transport has also been successful for the less conductive samples. In this case we preferred the superposition of two parallel mechanisms, both with their temperature range of significant contribution, instead of an abrupt change when the first one would be replaced by the second one. But at this point still one fundamental question remains unanswered; which is the 'true' mechanism or what is the physical relevance of the obtained parameters. Firstly, there is a dilemma when γ is 0.5 as it is common for several models. Secondly, both fits provide the eye-candy results and γ is the only one parameter which can be directly and immediately refused. Behind the rest parameters there are some microscopical details hidden such as the width of a potential barrier, the localization length, etc. We can at least note that values of T_0 and T_1 for the FIT model and their ratio are in the same order as obtained i.e. for PA [16]. On the other hand one could expect T_0^{FIT} a little bit higher as for $T \gg T_0$ the FIT becomes the ARH. The activation energies can be calculated from T_0^{ARH} and they are about 10^{-2} eV but since the ARH is a very general formula its origin is difficult to determine. The values of T_0^{γ} seem to be reasonable within both the CELT and the Q1D VRH models [18,51].

Nevertheless, to give a truly correct answer, at least two more things should be done: the extention of the measurement to the lower temperatures (close to liquid helium) where models can be easier distinguished, and provide other independent measurements that could quantitatively determine parameters. Both are beyond of the scope of this work. At this point we are just trying to confine ourselves to a hypothesis that as the composites contain truly metallic regions of Ag aggregates (except those theoretically possible from the ordered crystalline PANI regions) that are sufficiently large and not too separated, the FIT model might be preferred for the higher con-

ductive samples with a possible transition to the CELT when the metallic grains are smaller or the barriers are wider for the less conductive samples.

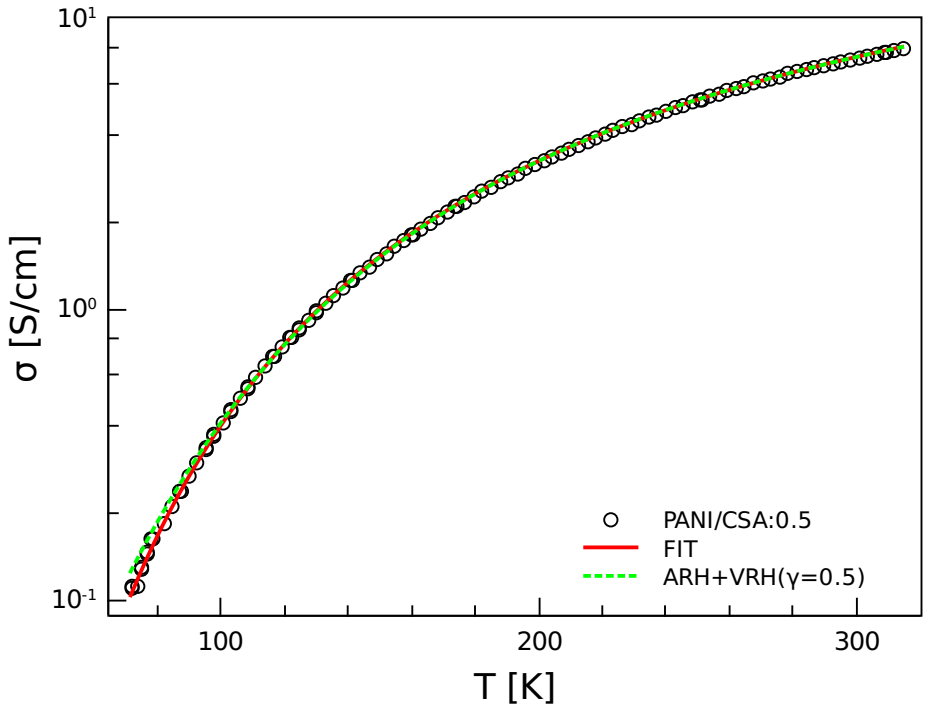

Figure 4.6: An example of the theoretical fit, PANI/CSA:0.5.

sample	σ_0^γ [S/cm]	T_0^γ [K]	σ_0^{ARH} [S/cm]	T_0^{ARH} [K]	σ_0^{FIT} [S/cm]	T_1^{FIT} [K]	T_0^{FIT} [K]
PANI/FA:1	580	2900	120	505	290	610	37
PANI/TSA:1	49	4700	1.7	360	4.5	560	23
PANI/SFA:1	16	1600	150	550	170	610	16
PANI/CSA:0.5	43	2500	32	550	49	630	30
PANI/CSA:0.5(N)	250	12600	3.5	720	64	1400	50
PANI/CSA:0.75	8.8	8500	0.42	1100	0.94	1030	48
PANI/CSA:1	45	4900	6.9	670	18	850	45

Table 4.3: The results of theoretical models fit for semiconducting samples.

Finally, we have to point out that there are macroscopic inhomogeneities on the surface, which are mostly of silver. This can be reflected on the experimental data apart from the microscopic structure.

4.1.3 Time dependences at constant T and p

In this type of experiment, changes in conductivity in vacuum were studied in respect to time. The general conditions have already been discussed in the previous chapter, we only remark that the pressure and the temperature were almost constant during the measurement, after about 1500 s when vacuum was achieved. Both, semiconducting and metallic samples were investigated and the influence of the dopant molar concentration was studied.

As it is shown on fig. 4.7, for all semiconducting samples, the conductivity was decreasing in time. In agreement with literature, e.g. ref. [34, 52], we suppose that this phenomenon is caused by losing moisture in the samples which influences conductivity. The maximal drop was observed for TSA, ca 0.67 from the initial value. This does not seem to be the same issue for metallic-like samples PANI/AC-Ag and PANI/MSA-Ag where at the conductivity about 10^3 S/cm it seems to be reasonable to suppose that the moisture does not contribute significantly to the overall transport but in the case of MSA water even inhibits transport. We note that the observed differences should not be due to the different thickness of samples as it did not vary significantly (tab. 4.1). It is believed that after enough time the conductivity would reach its 'saturated' time independent value.

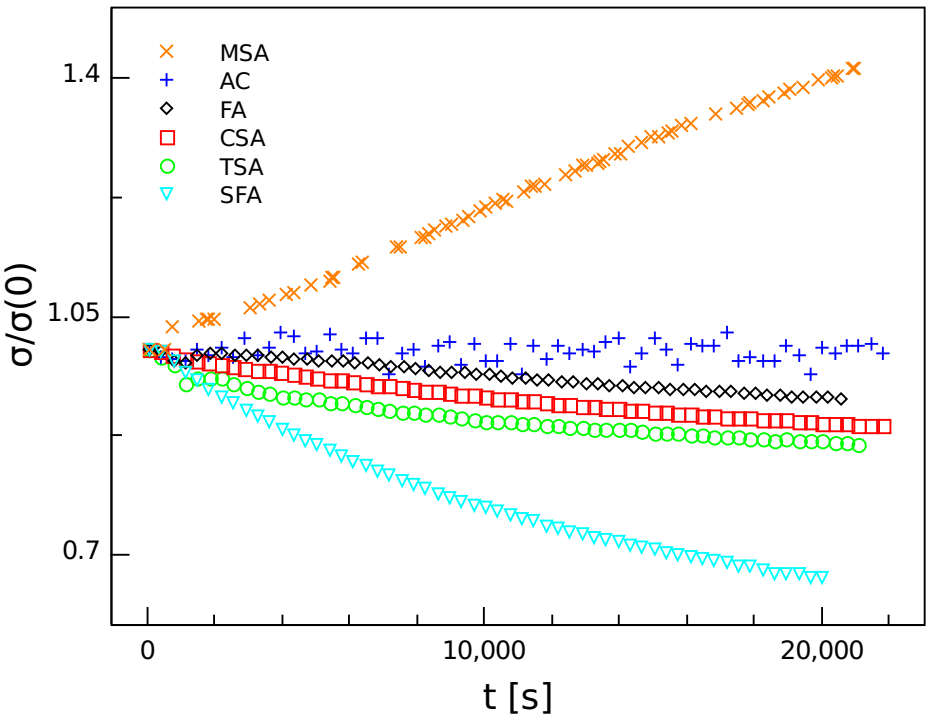

Figure 4.7: The time dependence of the conductivity PANI-Ag for different dopants at $M = 1$.

A relative change in the dependence on the molar concentration for CSA (fig 4.8) varies from ca 0.70 to 0.95% in respect of the initial value. In this case both samples from PANI/CSA:0.5 show similar behaviour (see discussion of the temperature dependence). Finally, all samples are less influenced than pure PANI/CSA. Metallic PANI/AC-Ag for this experiment shows the almost constant conductivity for all acid concentrations (fig 4.9). Surprisingly, the PANI/MSA-Ag conductivity increased in time and moreover, this behaviour is reversible (fig 4.10), what means that the first sight explanation based on the chemical structure changes (as some molecules with low molecular weight, i.e. acids, may escape from a sample) could be probably rejected. A hypothesis based on the morphology changes seems to be unlikely as well. One of the reasons could be that the presence of water molecules somehow breaks the charge transport down which is most probably driven by the silver nanoparticles. Nevertheless, this interesting phenomenon for sure deserves a further investigation.

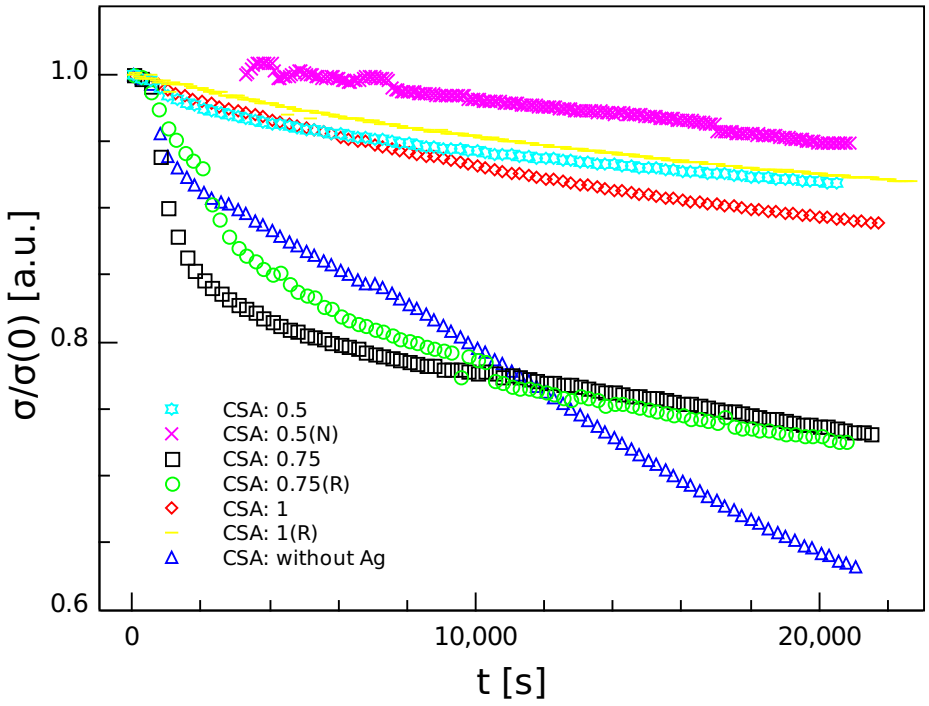

Figure 4.8: The time dependence of the conductivity PANI/CSA at different molar concentration.

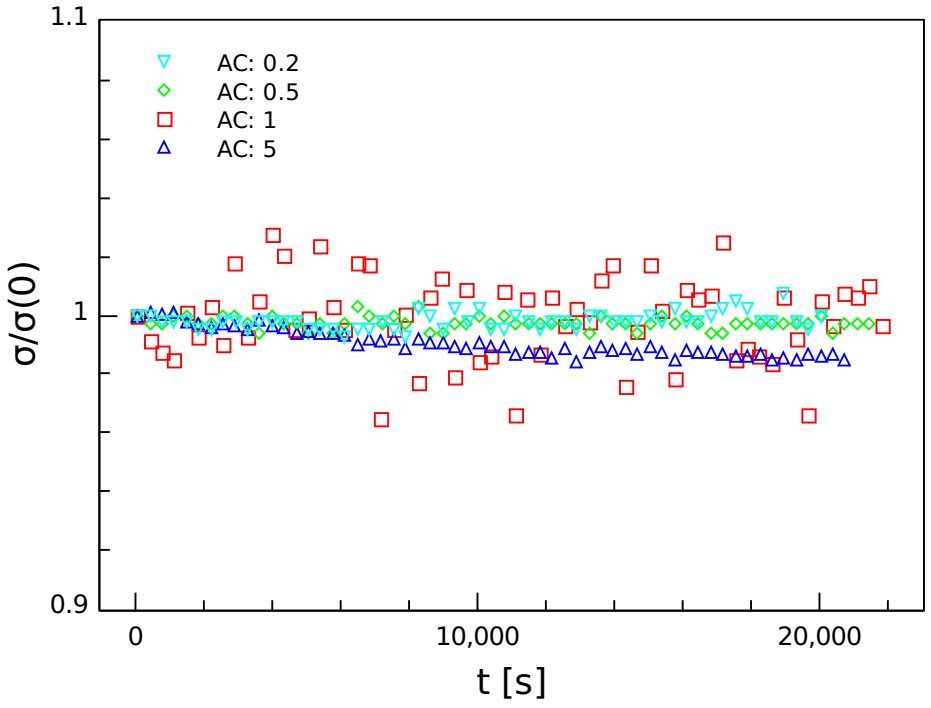

Figure 4.9: The time dependence of the conductivity PANI/AC-Ag at different molar concentration.

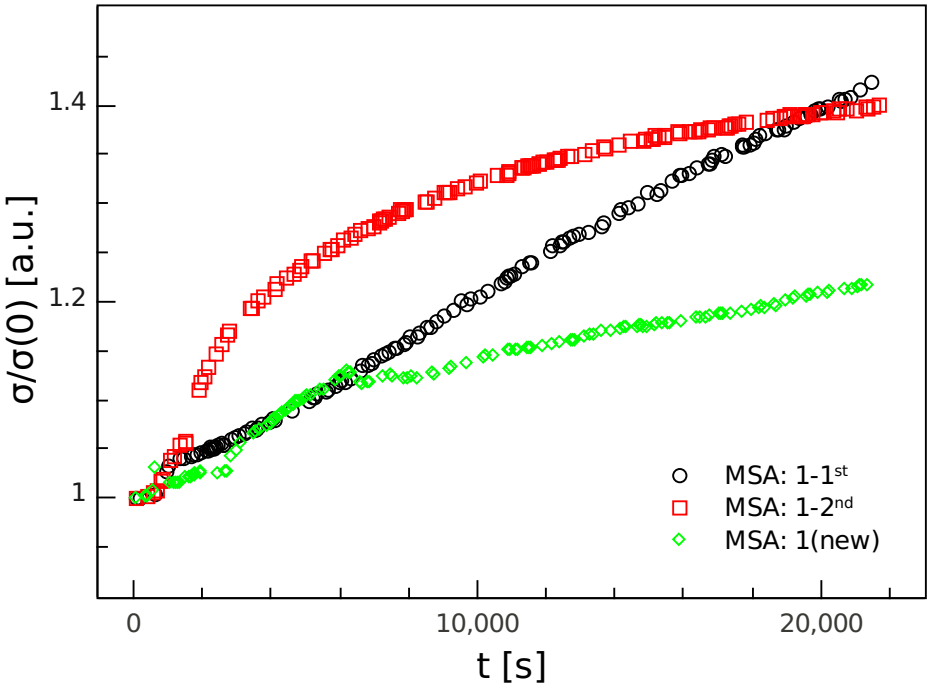

Figure 4.10: The reversibility of the time dependence of the PANI/MSA-Ag conductivity.

4.1.4 Effect of ageing

The room temperature conductivity for selected samples was remeasured after approximately two years in order to find out the effect of ageing in the composites. The table 4.4 shows there is no significant change, the relative decrease is not higher than 10 % ,thus we conclude that these composites are more stable that the pure PANI samples, where the conductivity decreased few orders of magnitude (though samples were treated at the higher temperatures) and as the reason of ageing a growth of amorphous phase at expense of the 'conducting islands' was suggested [53]. According to this picture a better stability of composites can be understood mainly from the different nature of the conducting islands - the silver nanoparticles that do not have to incline to ageing so much. This might be successfully used in applications. Moreover, despite of the mechanically damaged surface where the macroscopic breaches and inhomogeneities were observed by an optical microscope (fig. 4.11) the electrical stability does not seem to be influenced a lot.

sample	$\sigma^{orig.}$ [S/cm]	σ^{aged} [S/cm]
PANI/AC:1	3560	3530
PANI/TSA:1	1.4	1.3
PANI/CSA:1	1.7	1.5
PANI/CSA:1(R)	1.1	1.5
PANI/CSA:0.5	8.9	7.1

Table 4.4: The stability of the room temperature σ_{DC} at ageing of about two years.

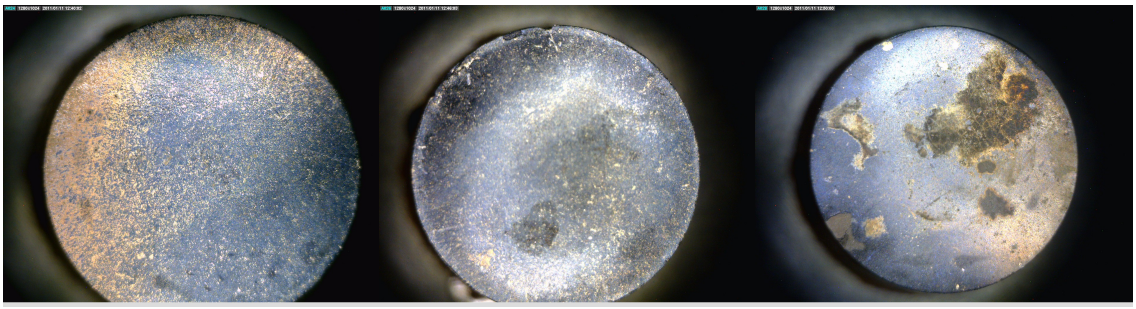

(a) PANI/CSA:1 (b) PANI/CSA:1(R) (c) PANI/TSA:1

Figure 4.11: Defects and inhomogeneities on the surface of selected pellets (after 2 years).

4.1.5 Conclusions

In this section we were investigating the electrical behaviour of PANI-Ag nanocomposites. They show both, the metallic-like temperature behaviour in the case of more conductive samples where AC and MSA were used as dopants, and the semiconducting behaviour in the case of less conductive samples doped with the rest of chosen

acids. There has also been discovered the influence of molar concentration of dopant in the case of PANI/AC-Ag samples which together with appropriate acid selection could be possible to use for the "tuning" of value of the electrical conductivity as well as its temperature dependence while concerning limitations provided by the chemical nature of the process. Less conductive samples also show a decrease in conductivity in time while facing lower pressures. This is believed to be caused by the moisture loosing in agreement with the literature and indicates PANI significant influence on the composite. On the other hand, the high conductive samples with AC as dopant are stable from this point of view. Although for MSA even increase of conductivity was observed and by this time any satisfactory explanation has not been found what, at least, makes it attractive for further investigation.

Since conductivity varies in several orders of magnitude and the temperature behaviour, both components, silver and doped polyaniline, seem to play an important role in overall charge transport mechanism. A determination of the theoretical model, well describing this phenomenon, is a rather complicated problem and in this case difficult to obtain. Behind that is lying not only a few experimental data (in term of good statistics), experimental limitations and a lack of theoretical models for these rather complex systems but we should also keep in mind that the final properties vary for the samples prepared at the same initial conditions, thus the technology plays a crucial role in order to achieve a reproducible behaviour. Despite of these limitations we have tried to give the basic insight by fitting current theoretical models. In the case of the metallic samples a linear function for resistivity has been successfully used, at least in a short temperature range and the thermal coefficient of electrical resistivity was determined. For the semiconducting samples fluctuation-induced tunnelling model as well as a superposition of the thermally activated transport and a model with soft-exponential dependence with coefficient 0.5 were successfully fitted. From the structural point of view and the better fit reliability the FIT model is preferred but the superposition of thermally activated the ARH model and the CELT model is not excluded and the transition from the FIT to the CELT could be possible for the less conductive samples.

Except the lack of theoretical explanations of transport mechanisms in compounds where metals form aggregates at nanometric scale in semiconducting matrix with hopping-like transport often preferred; other questions remain open as well: how the same amount of silver and more or less the same morphology (spherical nanoagregates of silver dispersed in polyaniline matrix) for all sulphonic acids doped samples is related to differences in orders of magnitude in electrical conductivity and different temperature behaviour, and why acetic acid provide formation of silver nanorods.

Finally, this field of study is still rich in the scientific and the technological challenges and it is worth to going on further with investigation. These novel and exciting materials promise us both, an intellectual and an application-like reward.

4.2 Polyaniline-montmorillonite composites

4.2.1 Introduction

In this section composites based on conducting polymer - polyaniline and insulating[6] part - montmorillonite (MMT) are studied. As mentioned previously (the section about PANI), the mechanical properties of PANI are in general not good enough for its applications. Several papers have been published about PANI/MMT composites declaring improvements in the properties or studying the structure-property relationship, i.e. [54–59].

First of all, MMT itself referred as a 2:1 phillosilicate is a member of the layered silicate clays family. The layers are in parallel alignment and they are attracted by the van der Waals force and the interlayer space can be filled by adsorbed cations, e.g. Na^+. MMT is usually used as a sorbent of organic compounds and can be mixed with polymer materials. According to the organic-inorganic components interaction, there are three different final states usually recognized, from intercalated composite where polymers are located between layers, through a flocculated state, to exfoliated composite where silica layers are separated and dispersed in polymer matrix [54]. While blending with PANI an improvement of the properties have been achieved, for instance, PANI/MMT composites based conductive coatings show a longer lifetime than PANI coatings [54], intercalated PANI/MMT composites are thermally more stable than pure PANI [55] or the mechanical properties were improved as the Young modulus is higher in the composites than in pure MMT [56].

The electrical properties of PANI are determined by its polaronic structure and hopping-like or conductive islands models are widely used, as stated before, with the room temperature conductivities ca 10^0 S/cm [34], whereas MMT belongs to ionic materials with conductivities from 10^{-5} to 10^{-10} S/cm [60, 61]. But the final properties of composites are determined not only by the properties and the morphology of their individual components but strongly depend on the structure of composites as well. It has been shown that the PANI chains intercalated among MMT crystalline layers increases the conductivity in respect of MMT and the conductivity is changed from an ionic to a pure electronic [57]. The mechanism of transport could be then described by the Q1D VRH where the layers of MMT can be considered as barriers blocking the interchain PANI transport [58, 59]. It was shown that conductivity strongly depends on the concentration of conductive part dispersed in insulating part and varies in several orders of magnitude [59].

Our research is based on samples of different composition (0,5,..,100); as the composition we consider both the mass of MMT per 100 ml of reaction mixture and wt%

[6] insulating in respect of PANI because MMT itself shows ionic conductivity

(vol%) of PANI in the composite (see a discussion below), different origin of MMT (Cloisite-CL, Belle Fourche-BF, Ivančice-IV) and different approach at their preparation (A,B). The samples were prepared[7] in two ways: either by the polymerisation of aniline hydrochloride with ammonium peroxydisulfate in aqueous suspensions of MMT (set A) what provided mainly surface polymerisation or by the intercalating polymerisation (set B), driven by a standard chemical reaction (fig. 1.2) with HCl as dopant [36]. The morphology of composites was investigated by the scanning electron microscope and mainly PANI coatings on the MMT surface were found without any presence of free PANI precipitates and any considerable differences between these coatings in respect to the way of polymerisation or the origin of MMT were not observed [36]. Both, the DC and the AC conductivity characteristics were obtained using different methods and devices: the VdP method in AC and DC regime, an electrometer, a LCR meter and a dielectric α-analyser. More details about techniques and experimental setup were given in chapters 2 and 3.

In the frame of this study we aimed to investigate an influence of three factors, mentioned above, on the electrical properties of composites. We also tried to find the charge transport mechanism in a material and compared the results from two different experimental methods.

4.2.2 Room temperature $\sigma_{\mathbf{DC}}$ and its ageing

The DC conductivity measurements at a room temperature show its strong dependence on composition. To avoid a misunderstanding, foremost, we refer the sample names, that are used throughout the work and reflect the composition, to a physical quantity - the mass of MMT in reaction mixture (table 4.5) [49].

sample name	$m_{MMT}[g]$
PANI: 100	0
PANI/MMT: 50	2
PANI/MMT: 33	4
PANI/MMT: 25	6
PANI/MMT: 20	8
PANI/MMT: 15	10
PANI/MMT: 10	18
PANI/MMT: 5	38

Table 4.5: A correspondence of the sample names used in the work and a physical quantity - the mass of MMT per 100 ml of reaction mixture [49].

[7] the Institute of Macromolecular Chemistry of Academy of Sciences of the Czech Republic, Prague

A real content of PANI in composites was obtained by TGA [36]. But the TGA results in contrary to the expected values (according to a monotonous function of MMT mass in reaction mixture) show the monotonous behaviour only for MMT-Cloisite set. For the rest of them there are such deviations that one could not more expect the final content of PANI only from the initial conditions. Moreover, the content of PANI remained unknown for all samples 15 and 20 and in the case of PANI/MMT(CL) it was at least interpolated to obtain a full data set. Further, the weight content was used to calculate a volume content of PANI in PANI/MMT(CL) composites while other estimations in the density were made. We would like to note that these issues strongly complicated a possible evaluation in respect to the concentration of the conductive phase in composite.

The results from the VdP measurements are plotted in fig. 4.12-4.13. A rapid monotonous change of conductivity in several orders of magnitude, $10^{-6} - 10^{0}$ S/cm, in respect to the mass of MMT can be noticed. One may suppose that this behaviour could by explained by the percolation as it was stated earlier. The non-monotonous behaviour of the PANI content indicates a hypothesis that the key parameter would be rather mass of MMT and, in principle, it could be related to the amount of amorphous barriers even for the same content of PANI. Nevertheless, the standard percolation formula (1.31) in respect to the conductive PANI phase content for PANI/MMT(CL) was tried to fit data but without a success. It seems that the 'transition area' is too wide, from 2-18 g of MMT (samples PANI/MMT: 10-50; resp. 26-50 vol.% of PANI in PANI/MMT(CL):A). Hence, we conclude that the observed behaviour can not be described within the classical percolation theory. But on the other hand, also more experimental data in terms of good statistics and a fine step in MMT mass would be helpful in a deeper analysis.

Following our goals, the way of the polymerisation probably does not influence the conductivity and the differences among montmorillonites are higher in the PANI content than in the conductivity. The small differences can be observed only in the transition region but even these do not have to be subscribed to the origin of MMT but rather we should consider them as a feature of the region (in a terminology of the percolation theory) where complete conductive paths are not yet established and thus the total conductivity can vary within orders of magnitude from sample to sample.

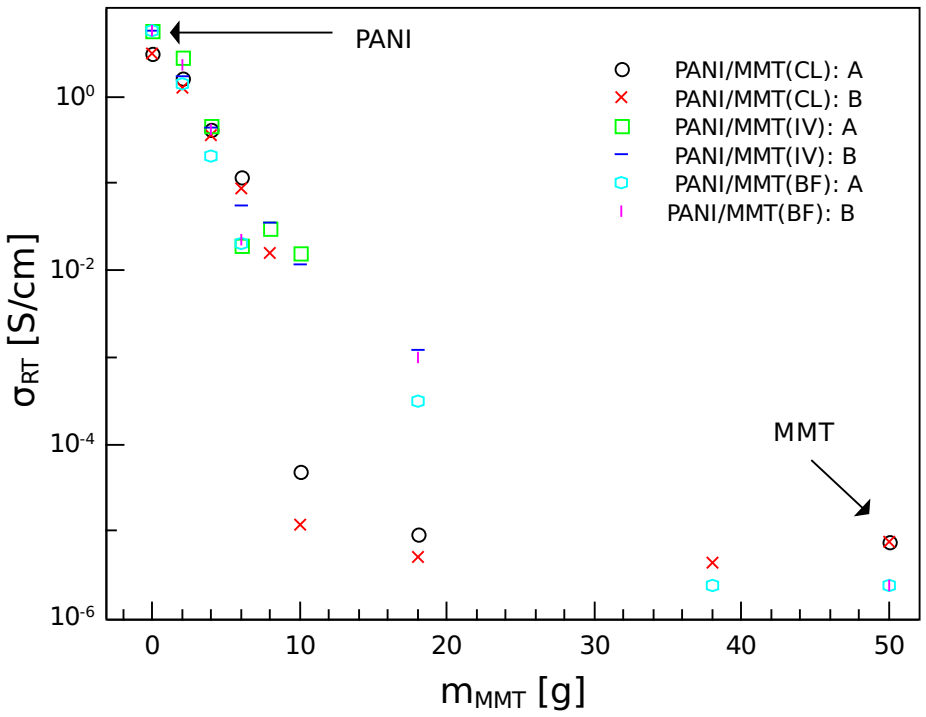

Figure 4.12: σ_{RT} from the VdP measurements for different origin and content of MMT in PANI/MMT.

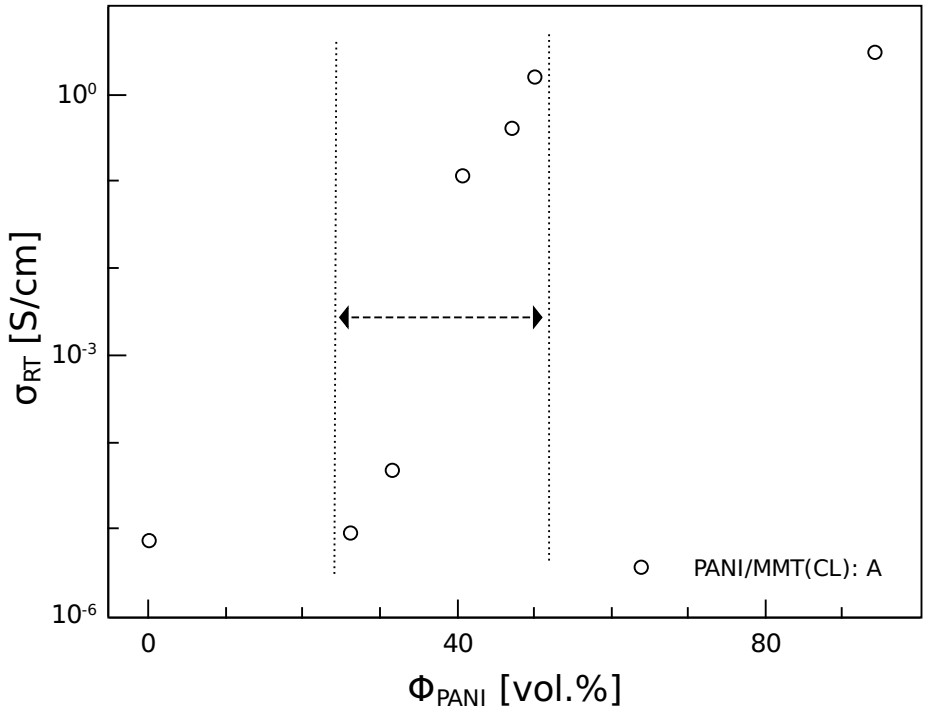

Figure 4.13: The dependence of σ_{RT} on the PANI content in PANI/MMT(CL).

We also studied the effect of ageing (tab. 4.6) for selected samples at room temperatures. The conductivity decreased maximally 25 times and the ageing effect is weaker for pure PANI. From the material science and the technological point of view this is not satisfactory as composites should have at least equally good properties as unmodified components (PANI in this case). The reason for the degradation of samples could be either on a structure level, as the degradation of PANI [53], or the morphology of PANI in composite. We attach some images (fig. 14.14) from an optical microscope in order to show macroscopic damages on the surface of samples. But in contrast to the conductivity measurements there are more defects in samples with the higher stability and thus it seems that the (surface) macroscopic defects are not responsible for observed differences in the conductivity.

sample	$\sigma^{orig.}$ [S/cm]	σ^{aged} [S/cm]
PANI	3.1	2.2
PANI/MMT(CL) A50	1.6	0.40
PANI/MMT(CL) B50	1.3	0.39
PANI/MMT(IV) A33	0.47	0.019
PANI/MMT(IV) B33	0.45	0.083

Table 4.6: The ageing effect on the room temperature σ_{DC}, the VdP data.

(a) PANI (b) PANI/MMT(CL):A50 (c) PANI/MMT(CL):B50

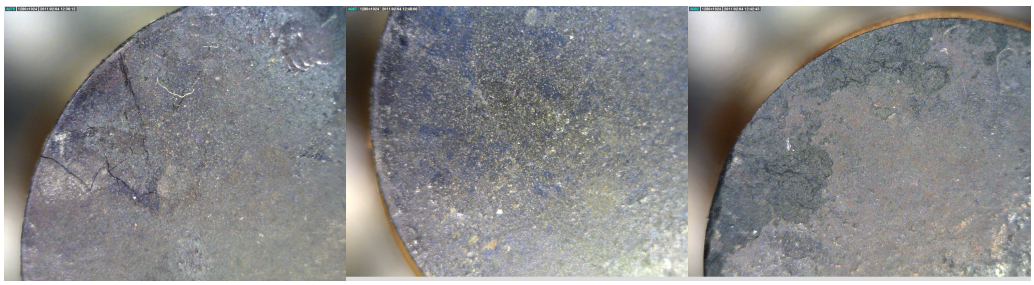

(d) PANI/MMT(IV):A33 (e) PANI/MMT(IV):B33 (f) PANI/MMT(CL):B25

Figure 4.14: Defects on the surface of pellets, an optical microscope, magnitude of 60 times.

4.2.3 Temperature dependences of σ_{DC}

The temperature dependence of σ_{DC} in the VdP configuration was investigated for sets PANI/MMT(CL):A,B and PANI/MMT(IV):A and the results are plotted as a relative change to σ_{300K} vs. T at fig. 4.15-4.17. There could be a general qualitative comment made that samples with the higher content of MMT (samples 15, 20, 25, 33) shows not only the lower absolute values of the conductivity but the relative change with decreasing temperature as well, in a comparison with pure PANI or PANI/MMT:50. The results also imply that neither the way of the polymerisation nor the origin of MMT play a significant role in a charge transport as they give very similar results.

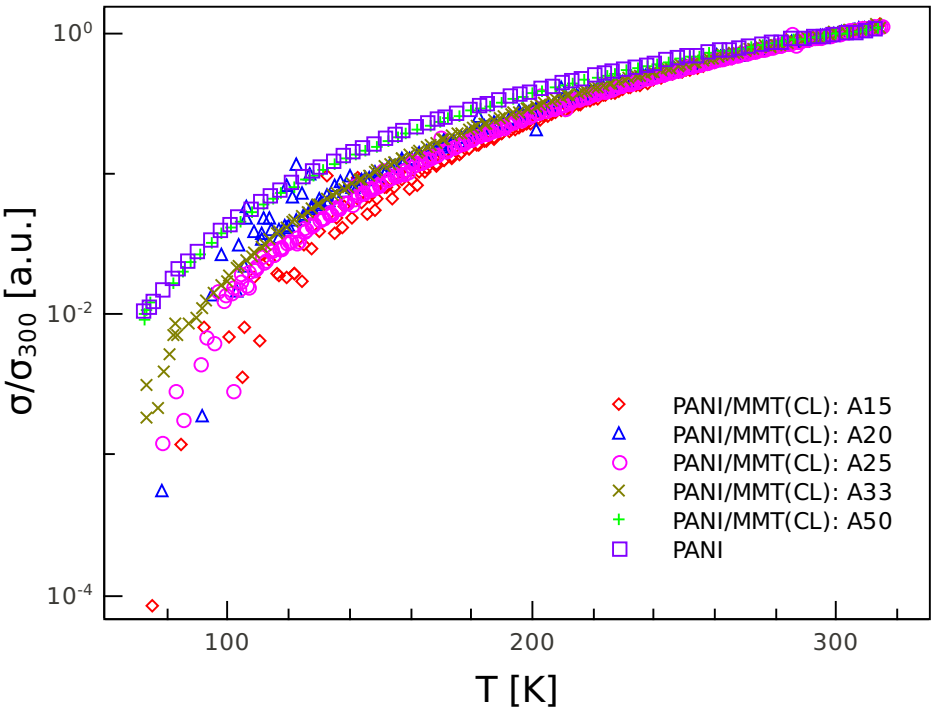

Figure 4.15: The temperature dependence of σ for PANI/MMT(CL):A set.

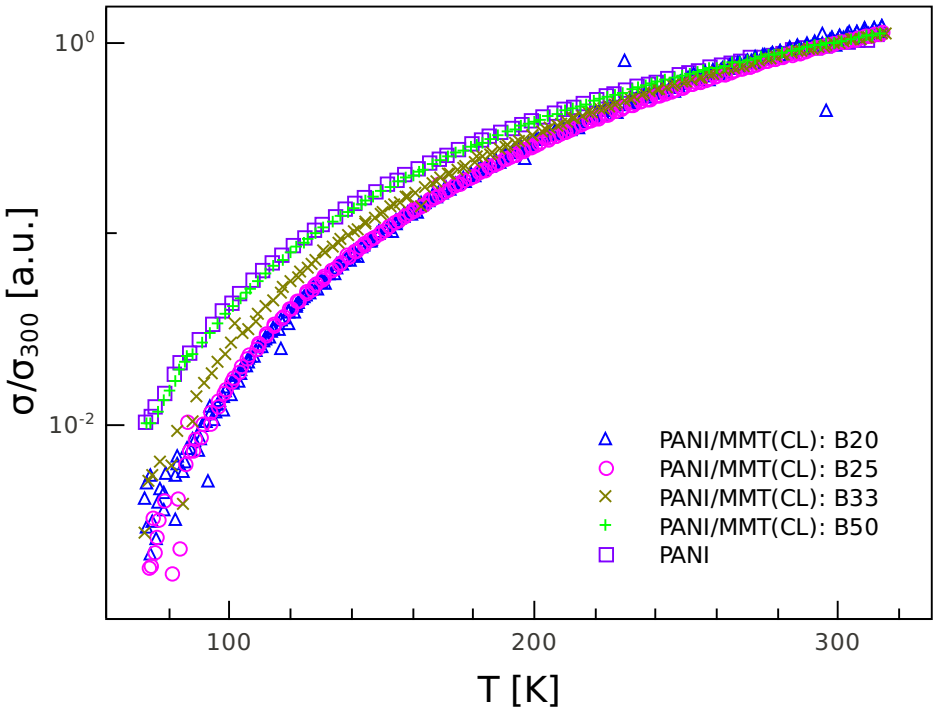

Figure 4.16: The temperature dependence of σ for PANI/MMT(CL):B set.

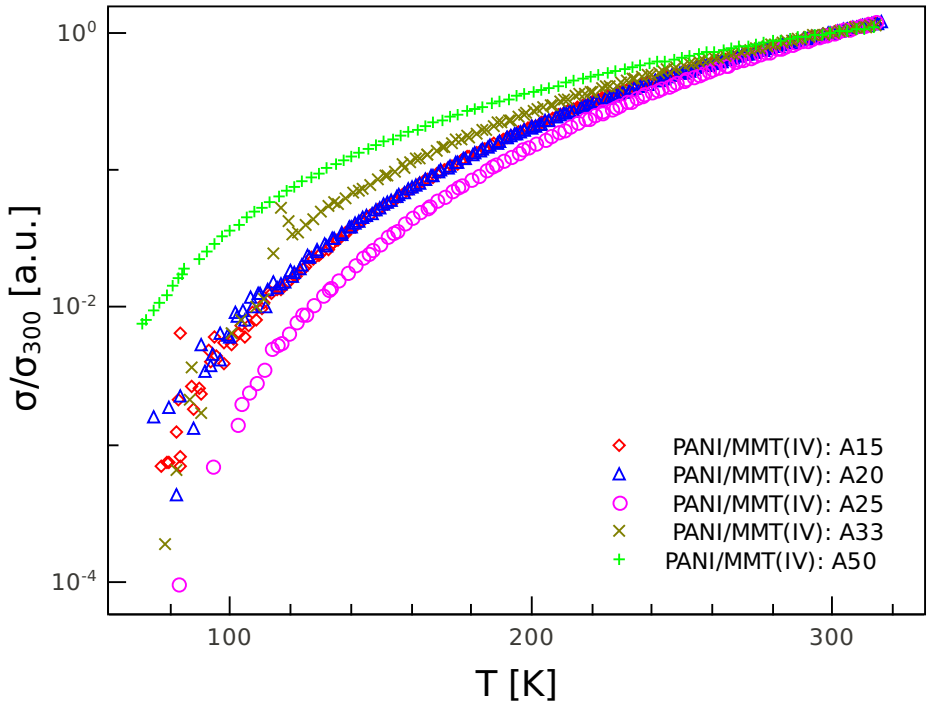

Figure 4.17: The temperature dependence of σ for PANI/MMT(IV):A set.

The quantitative analysis was also done where possible. The experimental data were fitted[8] using equations for following models: the VRH-like (eqn. 1.24), the FIT (eqn. 1.27) and the ARH-like (eqn. 1.18) thermally activated transport. While taking a full temperature range (ca 80-315 K) into account and one theoretical model, then any of the proposed models could not satisfactory describe the experimental data. The results of the VRH fit with exponents 0.25 and 0.4 according to ref. [14] gave unrealistic values of the parameters with no agreement neither at low temperatures nor at high temperatures. From this 'battle' the best model is the VRH with $\gamma = 0.5$ which deviates mainly at high temperatures. We noticed from $log\,\sigma$ vs. $1/T$ plot that for high temperatures (above ca 200 K) the ARH is more suitable. This, naturally, led us to an idea[9] supported by ref. [2] (but without the geometrical factor that would increase a number of parameters what is unwelcome, moreover it could be possibly counted within σ_0) that in such complex systems there could be more than one mechanisms which contribute to the overall transport. That is why we fitted a superposition of the two most appropriate mechanisms which successfully described measured data in almost whole temperature range. It is demonstrated for pure PANI sample in fig. 4.18. It also means that the type of transport is determined by PANI itself and the presence of MMT would then act as some effective barrier to the transport. This is reflected mainly in the values of fitted parameters (tab. 4.7). It has to be noted that even model of the FIT successfully described data in lower temperatures while standing alone but together with the ARH model it did not agree with the experiment at low temperatures as the VRH-like model did. Nevertheless, this difference was rather small and at temperatures under 100 K where measured data were often less reliable. Thus one can argue that the FIT model may not be excluded. Despite of that we continued only with the VRH-like ($\gamma = 0.5$) and the ARH model. At the same time we believe that the fit of more than two mechanisms would be useless due to more free fitting parameters. For the samples with the lower conductivity (samples 25 and lower) this evaluation failed giving enormous relative errors of the parameters (more than 100%) due to the unreliable data at low temperatures where the VRH-like model plays a crucial role. At least for the more conductive samples the parameters of used theoretical models were obtained.

As mentioned before, the VRH-like formula with exponent $\gamma = 0.5$ is quite general since it is derived for more than one transport mechanisms, thus only a fitting procedure alone can not decide which one of the transport mechanisms is responsible for the conductivity. Hypothetically, we can prefer the Q1D VRH arguing in terms of the material structure according to ref. [58] that the conduction is mostly provided by polyaniline chains which are separated by insulating MMT silica layers acting as barriers to the polaron transport. The PANI chains can traverse these barriers providing mainly the Q1D transport. However, other models like the CELT can not be just eliminated until the Q1D VRH is properly justified (i.e. by other different measurements). Within the Q1D VRH T_0^{VRH} parameter is linked with a recipro-

[8] used the Leverberg-Marquardt and the simplex method implemented in the program OriginPro

[9] the same approach than in the case of semiconducting PANI-Ag composites

cal value of the localization length in the system. In our system this parameter is increasing with a lower concentration of PANI in composite what means that the localization length becomes bigger, probably due to the lower content of conductive parts in insulating matrix. A similar situation is in the case of the ARH model since it covers a wide range of processes so it is difficult to decide what is its origin in this system. Finally, we note we are aware of the fact that instead of a superposition there could be fitted two processes independently with an abrupt change from the first to the second one model. This alternative approach can be understood i.e. when with temperature the Q1D VRH changes to the nearest neighbour hopping and the ARH gains form of eqn. (1.21) with T_0^{ARH} related to the largest barrier. In practice, only the parameters in table 4.7 would be changed but the basic question of the true origin of the transport would remain opened. We now see that a determination of the theoretical model is still a big challenge.

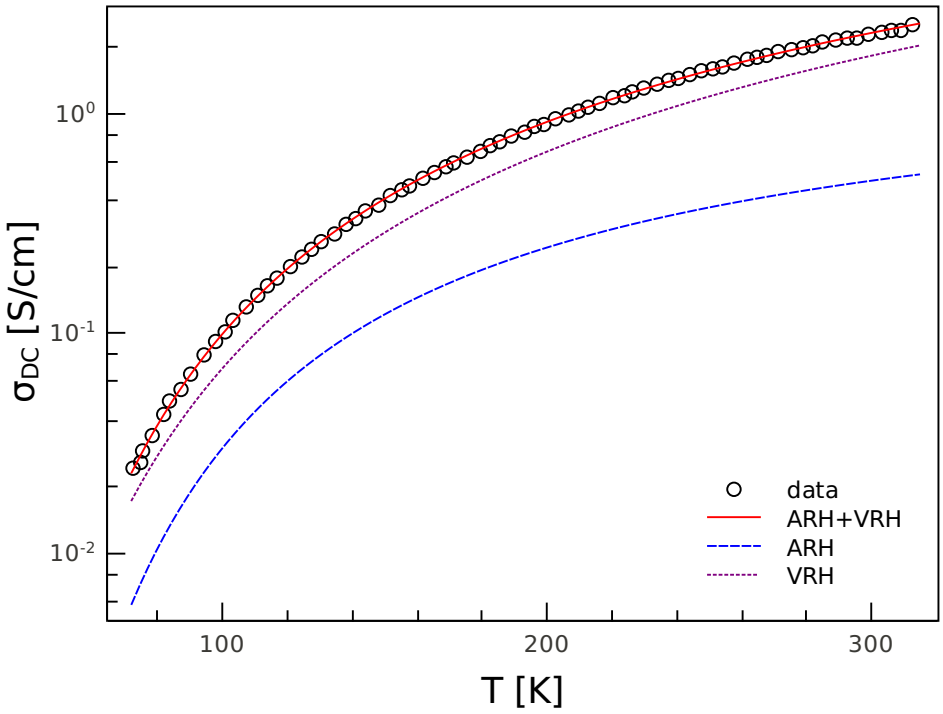

Figure 4.18: A demonstration of the superposition of the ARH and the VRH for sample PANI.

sample	σ_0^{VRH} [S/cm]	T_0^{VRH} [K]	σ_0^{ARH} [S/cm]	T_0^{ARH} [K]	E_a^{ARH} [10^{-2} eV]
PANI	160	6000	2	420	3.6
PANI/MMT(CL): A50	92	6900	0.6	370	3.2
PANI/MMT(CL): A33	73	9700	0.2	510	4.4
PANI/MMT(CL): A25	26	10400	0.06	850	7.3
PANI/MMT(CL): B50	84	7000	0.6	380	3.3
PANI/MMT(CL): B33	60	9700	0.3	440	3.8
PANI/MMT(CL): B25	14	9500	0.05	570	4.9
PANI/MMT(IV): A50	97	5900	1.7	560	4.8
PANI/MMT(IV): A33	27	9800	0.5	1010	8.7
PANI/MMT(IV): A25	9	19200	0.1	1200	10.3

Table 4.7: The parameters from a fitting procedure.

4.2.4 Time dependence of σ_{DC} at constant p and T

As noted previously, PANI/MMT composites contain water, about 6-8 % w.t. [36], which influences the charge transport [34]. Therefore the measurements at the constant temperature and low pressure (ca 10 Pa in our case) could be interesting. More details about the experiment were described in chapter 3, again the VdP technique was used. The results of the measurements are plotted at fig. 4.19-4.21. We can conclude that a general trend is the decrease of the conductivity as expected due to decreasing moisture in samples [34]. For PANI/MMT(CL) there are two exceptions 25 and 33, which show only a very gentle decrease for both sets A and B. Up to now, there is no a satisfactory explanation, and within our picture of the composites there is not any reason for a such exception. We only suppose that water molecules could be somehow trapped in the internal structure of composite and thus were not evacuated. Next, there is not any considerable difference in the results for sets A and B in any of the measured samples and we believe according to the results from the experiments of the temperature dependence of the conductivity, the way of composite preparation does not play any role in the transport mechanism. On the contrary, interesting seems to be that for PANI/MMT(IV) there is a stronger decrease in the conductivity (0.35 from $\sigma(0)$) in a comparison with PANI/MMT(CL) (0.6-0.7 from $\sigma(0)$) for all investigated samples; moreover the conductivity significantly drops for PANI/MMT(IV):A25 and A33 that only support our opinion that there is not any reason for the general exception for these compositions and the results for PANI/MMT(CL): A25, A33 are only a matter of coincidence and they are probably unreproducible.

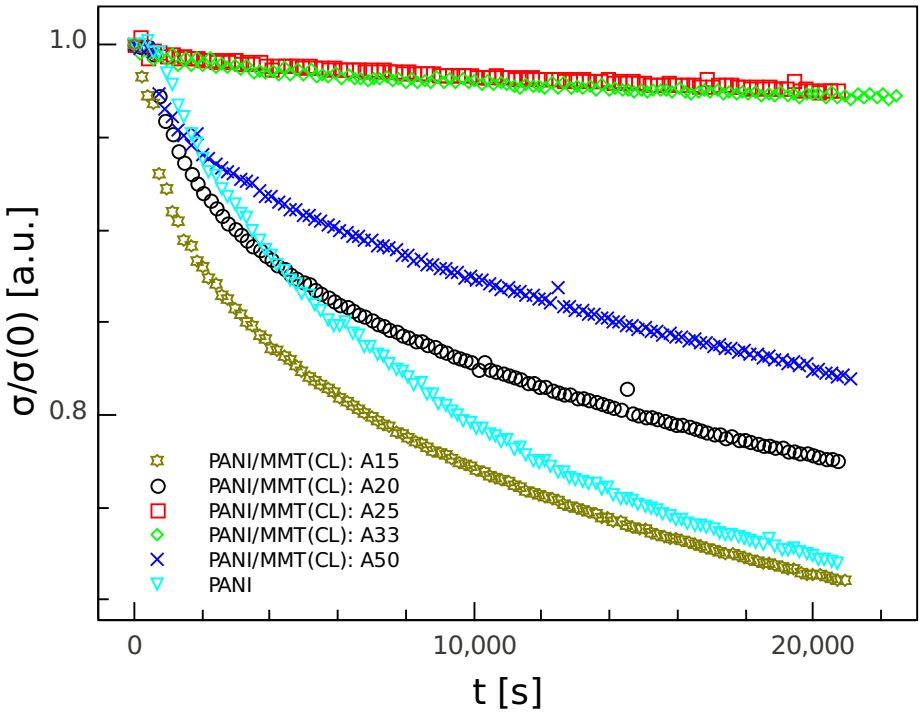

Figure 4.19: The time dependence of σ_{DC} for different m_{MMT} in PANI/MMT(CL):A.

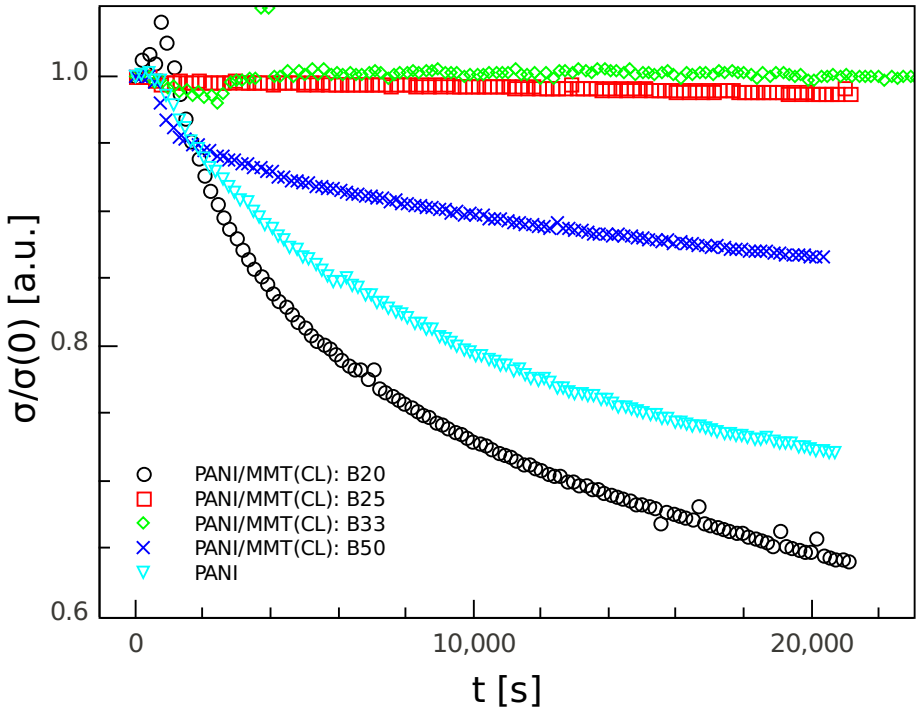

Figure 4.20: The time dependence of σ_{DC} for different m_{MMT} in PANI/MMT(CL):B.

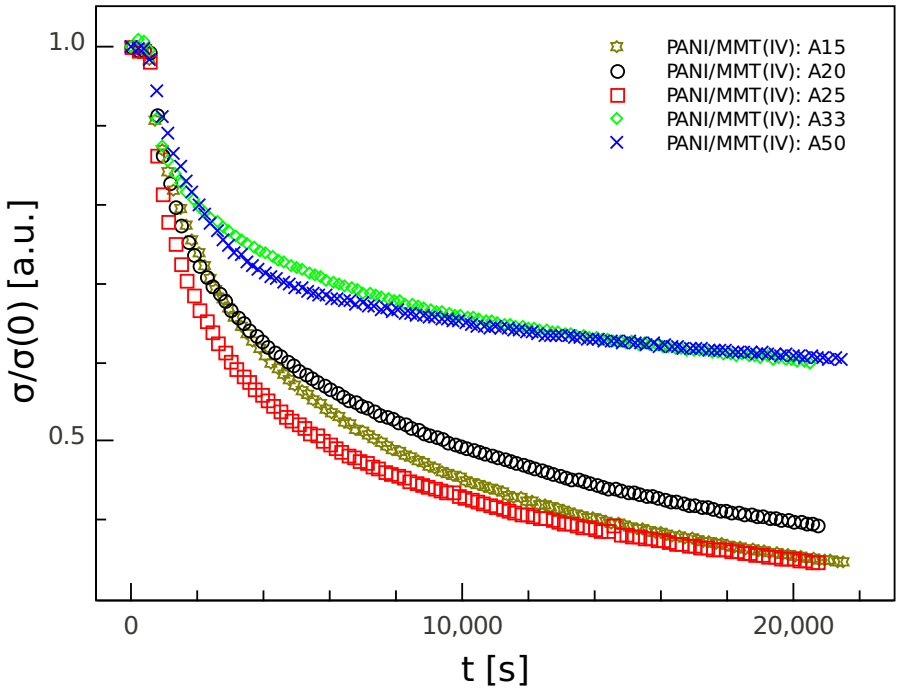

Figure 4.21: The time dependence of σ_{DC} for different m_{MMT} in PANI/MMT(IV):A.

4.2.5 Frequency dependent conductivity and dielectric spectroscopy

AC conductivity - van der Pauw configuration

In this paragraph we discuss the frequency dependent conductivity obtained for selected samples (aged ones) using the VdP method at a room temperature. Its dependence on the current was investigated and a comparison with σ_{DC} was made. We noticed that σ_{DC} is independent on the current for currents higher than 10^{-3} mA and even for lower currents the differences are rather small. But this is not so for σ_{AC}[10] where high currents at least 0.1 mA are essential otherwise there is a strong dependence on the measuring current giving arise to the differences in 3-4 orders of magnitude at currents ca 10^{-4}-10^{-5} mA (fig. 4.22). Hence, to obtain the consistent data as high as possible currents were chosen and the frequency spectra were measured limited by a device to frequencies of 3-10^4 Hz. The results for PANI/MMT(IV) B33 are plotted in fig. 4.24 as representative. Two features can be noticed. Firstly, σ_{AC} at these low frequencies remains constant and it is equal to σ_{DC} (plotted against frequency 0.1 Hz as it reflects a nature of the measurement) as expected for disordered semiconductors. Secondly, from frequencies in the decade of 10^2 Hz it falls what is against an expected increase following from the theory. As the experimental

[10]in this part we refer $\sigma_{AC}(\omega)$ as the real part of the complex conductivity $\sigma'(\omega)$

setup is not primarily intended for high frequencies the parasitic impedances could play a role and we suppose that the differences are due to the technical limit.

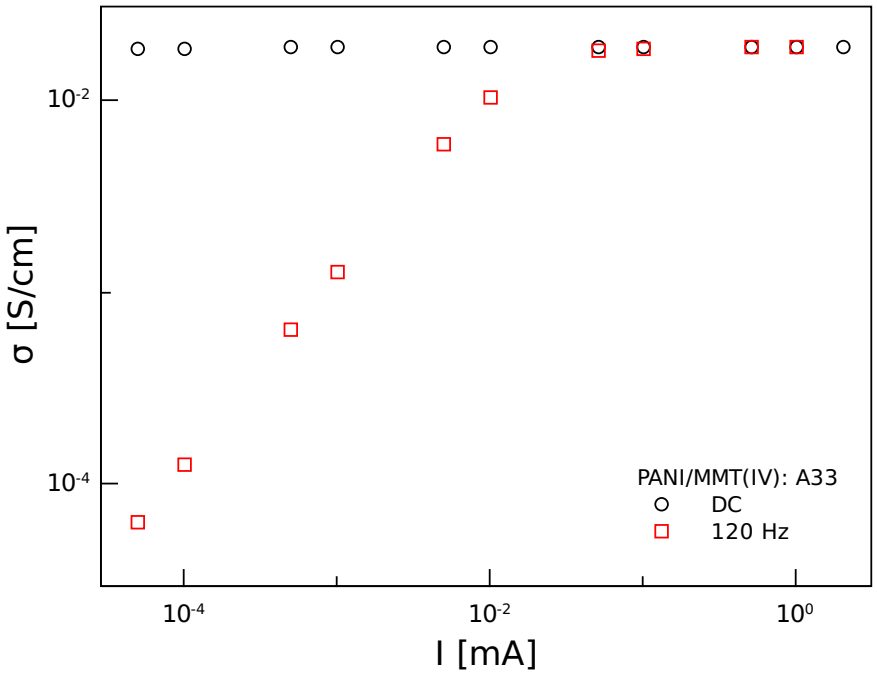

Figure 4.22: The current dependence of σ_{AC}. PANI/MMT(IV) A33 as representative.

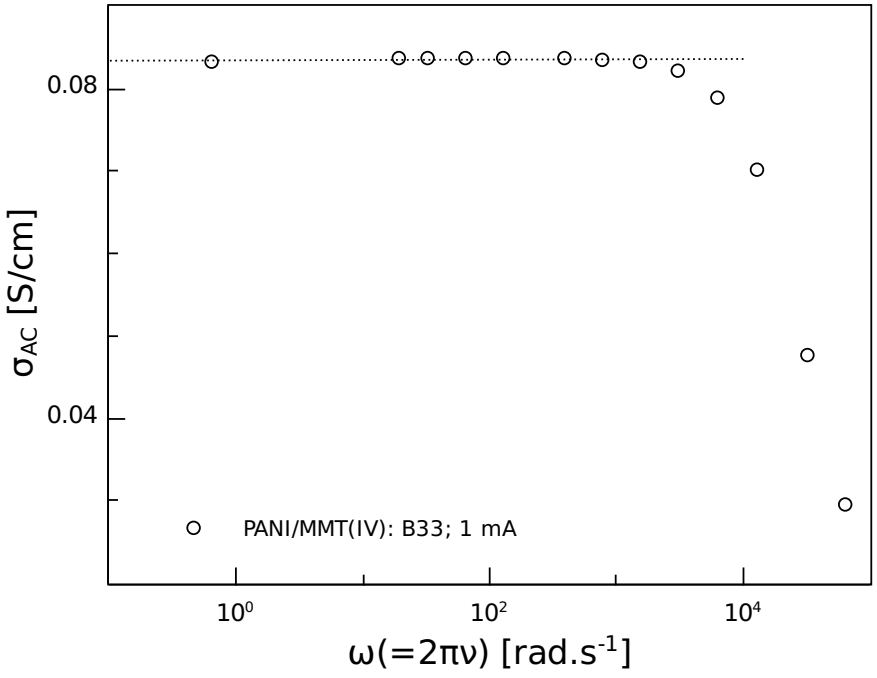

Figure 4.23: A frequency spectrum of PANI/MMT(IV) B33 as representative sample. The line is just a guide for the eyes.

AC conductivity - 'two-probe' technique

Again, as in the previous paragraph, the measurements were provided on samples that faced 2 years of ageing. Due to the different experimental devices limits (as we have discussed e.g. in the previous paragraph) two different devices, an impedance bridge and a dielectric analyser, were used in order to obtain reliable σ_{AC} data. The agreement was usually satisfactory except of high frequencies for high conductive samples PANI/MMT(CL): A/B50 where a similar effect of the conductivity drop as before was observed in the analyser measurements. But in this region the applied external voltage from the source could not be maintained properly what indicated that these data were not reliable and the impedance bridge was preferred. Moreover, it shows a limit of the dielectric analyser for high conductive samples and alternative techniques should be find in further investigation. In spite of this a frequency range of the impedance bridge is narrower than the dielectric analyser enables and for an evaluation, data from the later were preferred where it was possible. An electrometer was used to obtain values of σ_{DC}. Again, we can see (fig. 4.24) that in a low frequency regime there is a plateau and σ_{AC} is close to σ_{DC} and for higher frequencies an expected increase occurs. Also the imaginary part of the conductivity confirms a typical behaviour of disordered solids (fig. 4.25) [29]. At low frequencies the parasitic effect of the electrode polarisation can be identified.

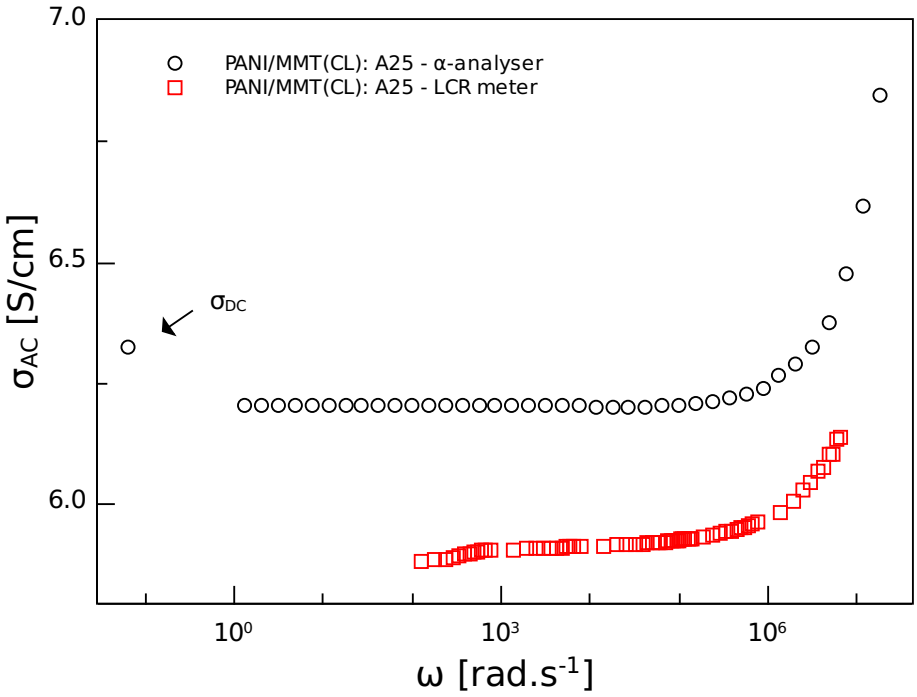

Figure 4.24: A frequency spectrum of PANI/MMT(CL) A25 at the voltage about 2 V as a characteristic behaviour.

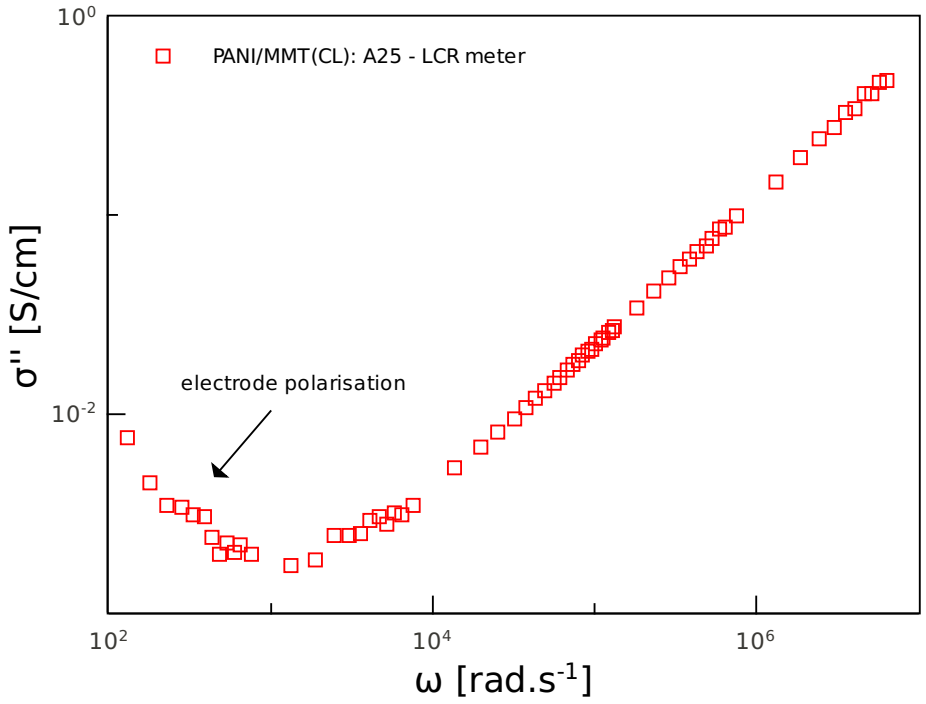

Figure 4.25: A frequency dependence of σ'' for PANI/MMT(CL) A25 at about 2 V.

A typical power law (eqn. 1.32) was fitted to the data firstly with the constant s and later with the frequency dependent s according to microscopical models described in chapter 1. It should be mentioned that only for few samples a fitting procedure was successful due to either unreliable experimental data or the combined dielectric response with the conductivity for less conductive samples and the possible polarisation effects at electrodes at low frequencies [62]. We fitted data in respect to three theoretical models, the universal power law (Joncher), the electron tunnelling and the random free energy barrier model (Dyre). The polaron tunnelling model completely failed. When we look at obtained parameters (table 4.8) it is obvious that the electron tunnelling and the free energy barrier model give unrealistic values of the phonon frequency in a comparison with the literature value $\sim 10^{13}$ [25]. At least σ_0 (σ_{DC}) was determined reliably since the mentioned plateau was extended to a wide frequency range. The values of ω_c lie above measured interval what implies that the observed increase of σ_{AC} can be just the part of the 'knee' and hence, further investigation should lead to a wider experimental frequency range.

All values of σ_0 are ca 1 order of magnitude lower than the DC conductivity measured by the VdP method. The similar results were obtained for PANI/MMT composites in ref. [61]. We believe that the samples were thin enough and that in both cases the bulk conductivity was measured. Probably in this material the conductivity is anisotropic and the transport is favoured in a perpendicular direction in respect to the probes. A frequency range for the VdP configuration was experimentally more

limited, therefore we have only a comparison within the plateau area in the low frequency regime.

sample	$\sigma_0[S/cm]$	$\omega_c^J[rad.s^{-1}]$	s	$\omega_0^E[rad.s^{-1}]$	$\omega_0^D[rad.s^{-1}]$
CL-A50	4.79×10^{-2}	1.2×10^{9}	0.94	6.9×10^{22}	1.9×10^{18}
CL-B50	4.06×10^{-2}	1.8×10^{9}	0.90	7.8×10^{25}	5.8×10^{19}
IV-A33	2.38×10^{-3}	3.8×10^{8}	0.86	3.3×10^{19}	3.1×10^{15}
CL-A25	6.20×10^{-4}	1.9×10^{8}	0.97	2.3×10^{22}	1.5×10^{18}

Table 4.8: The results of σ_{AC} fitting procedure. Indexes J, E and D stand for the Joncher's, the electron tunneling and the Dyre's model of a power law.

Using the α-analyser also the temperature dependence of σ_{AC} was measured and the conductivity approach was appropriate mainly for conductive samples such as A33, A25, A10. We note that these temperature characteristics were measured for original samples and can be possibly compared with the results discussed above only in the sense of ageing. Unfortunatelly, only teh data for A25 (fig. 4.26) were then fitted in respect to the universal law (Joncher) and the coefficient s was determined (table 4.9). Other models completely failed. Disordered solids which the universal law was proposed for generally give the exponent s smaller than 1 [29]. In our case $s > 1$ and the conductivity is higher than the exponent $s = 1$ would predict and there is maybe another contribution to σ_{AC} and more than one mechanism should be fitted. An alternative explanation is offered by the recent model based on the distribution of the conduction path lenghts which allows exponents higher than 1 [63]. Nevertheless, to give a reliable answer further research is needed.

$T[°C]$	$\sigma_0[S/cm]$	$\omega_c[rad.s^{-1}]$	$\omega_0[rad.s^{-1}]$	s
-160	3.22×10^{-7}	3.0×10^{4}	4.4×10^{5}	1.28
-140	7.59×10^{-7}	4.0×10^{4}	1.1×10^{6}	1.33
-120	1.54×10^{-6}	6.0×10^{4}	2.0×10^{6}	1.36
-100	3.48×10^{-6}	1.4×10^{5}	4.0×10^{6}	1.35
-80	6.88×10^{-6}	1.4×10^{5}	6.3×10^{5}	1.42
-60	1.35×10^{-5}	1.4×10^{5}	9.2×10^{5}	1.47

Table 4.9: The results of temperature dependendence of σ_{AC} fitting procedure for PANI/MMT(CL): A25.

The temperature dependence of extracted σ_0 is shown in fig. 4.27 where it is compared with the 'VdP values'. The differences are now more drastic than before, three orders of magnitude. It seems that the differences are only a slightly temperature dependent and the ratio of 10^3 can be expected for room temperatures as well. After two years it decreased to 10 so it seems that the possible anisotropy is reduced. Hypothetically this may be linked with the composite morphology, the more ordered phases in different directions change with time towards the more disordered state.

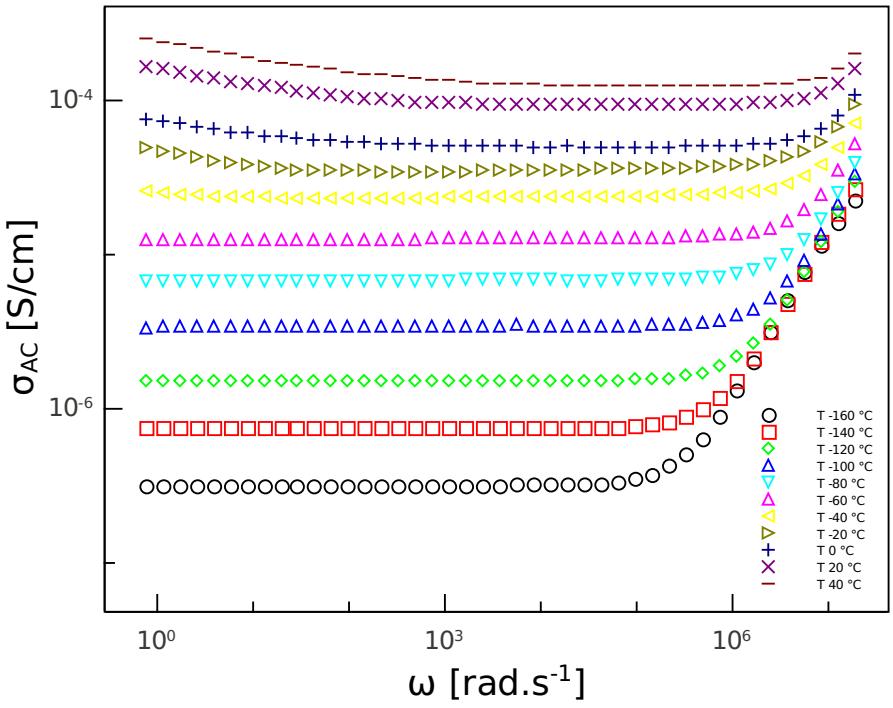

Figure 4.26: The temperature dependence of σ_{AC} spectrum. PANI/MMT(CL): A25.

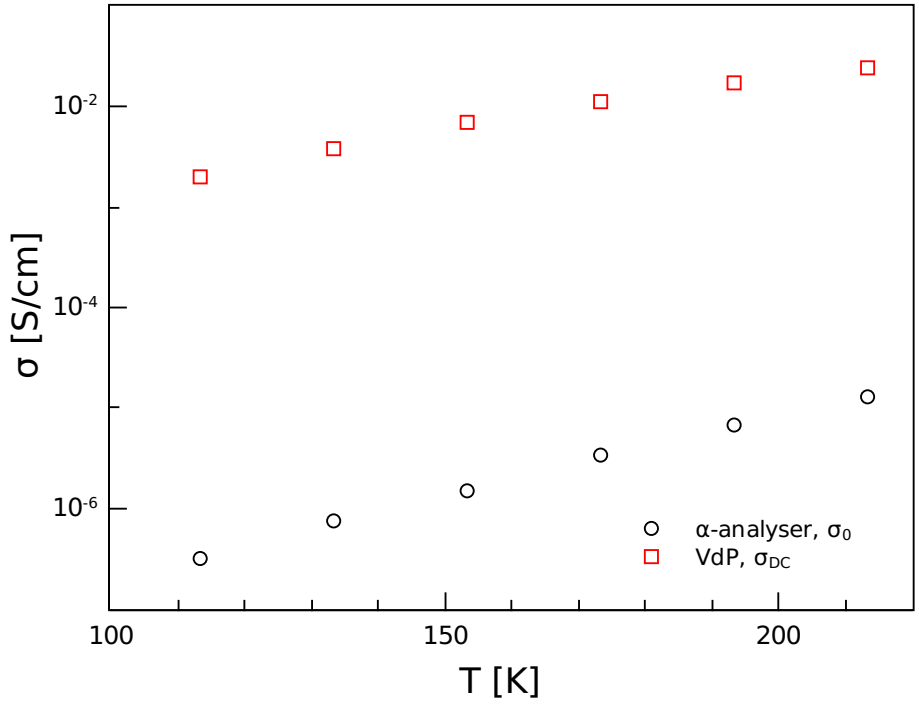

Figure 4.27: The temperature dependence of fitted σ_0 and its comparison with VdP σ_{DC} for PANI/MMT(CL): A25.

Dielectric spectroscopy

Within lower temperatures and for the more resistive samples a dielectric spectroscopy point of view was chosen providing an information about the relaxation processes in a material where the σ_{DC} contribution was significantly suppressed. But in general, we deal with the material where there is both, ionic and polaronic structure presented and the analysis went strongly complicated due to the parasitic effects such as the enormous electrode[11] polarisation at low frequencies (fig. 4.28) and may be also the Maxwell-Wagner-Sillars polarisation at the phase interfaces. Therefore the relaxation behaviour was successfully identified only in pure MMT(CL) and some from the PANI/MMT-5 samples. For the rest of samples a fitting procedure[12] failed either due to the high σ_{DC} contribution or the strong overlap of the relaxation processes. Despite the imaginary part ϵ'' contains the σ_{DC} contribution, it was successfully used instead ϵ' data that were completely unsuitable for fitting. However, the obtained fitting parameters give a rather rough picture than exact values. Samples PANI/MMT(CL): B5 and PANI/MMT(BF): B5 were chosen as representatives (fig. 4.29-4.30). On the former plot we can see two relaxation processes (the first one with broad and the second one with a narrow distribution of the relaxation times), which were fitted by the Cole-Cole equation (1.45) but obviously strongly overlap. On the later plot there is again at least one relaxation peak and with increasing temperature the significant contribution of conductivity appears at lower frequencies.

The results of fits are summarized in table 4.10. Temperature shift in the frequency maximum (fig 4.31) is well described by the Arrhenius equation and the activation energies for these processes were calculated. Fig. 4.33 shows the coefficient α of the Cole-Cole equation reflecting the distribution width of the relaxation processes. It should remain constant with temperature.

sample	$E_a[eV]$	α
MMT(CL)	0.50	0.45
PANI/MMT(CL) A5	0.04	0.45
PANI/MMT(CL) B5 p1	0.14	0.65
PANI/MMT(CL) B5 p2	0.25	0.3
PANI/MMT(BF) B5	0.53	0.69

Table 4.10: The activation energies and the distribution widths of the relaxation processes.

[11] for the high conductive samples such as A25 even negative values were measured, we do not present it here since it deserves much deeper investigation but in general it significantly complicates a quantitative analysis

[12] sincere thanks here to Ass. Prof. Jan Nedbal who is an author of the analysis software

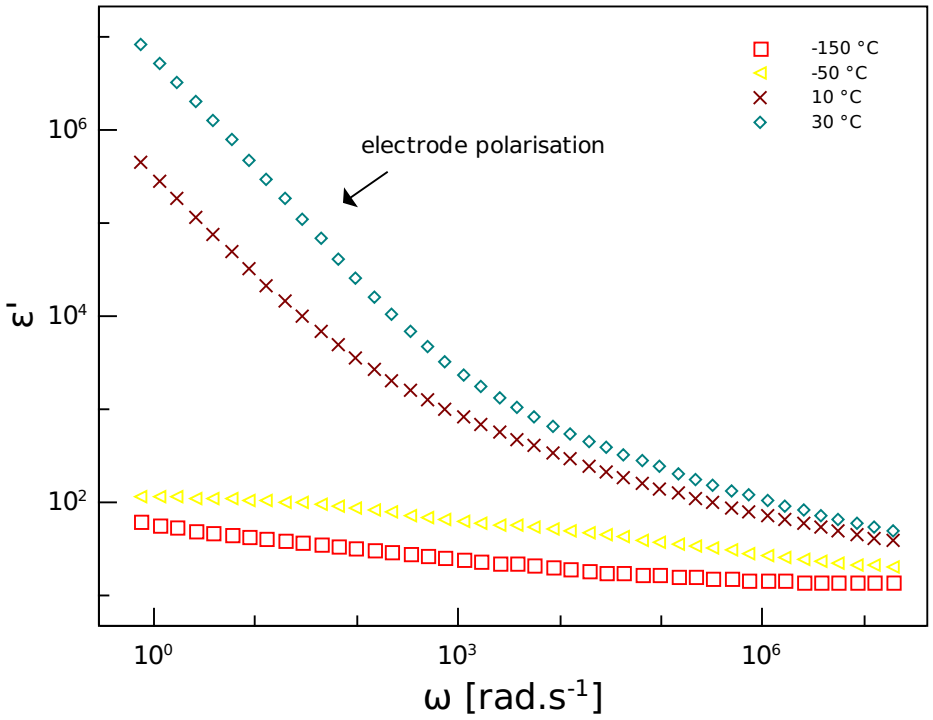

Figure 4.28: A dielectric spectrum of PANI/MMT(CL) B5, ϵ' plot.

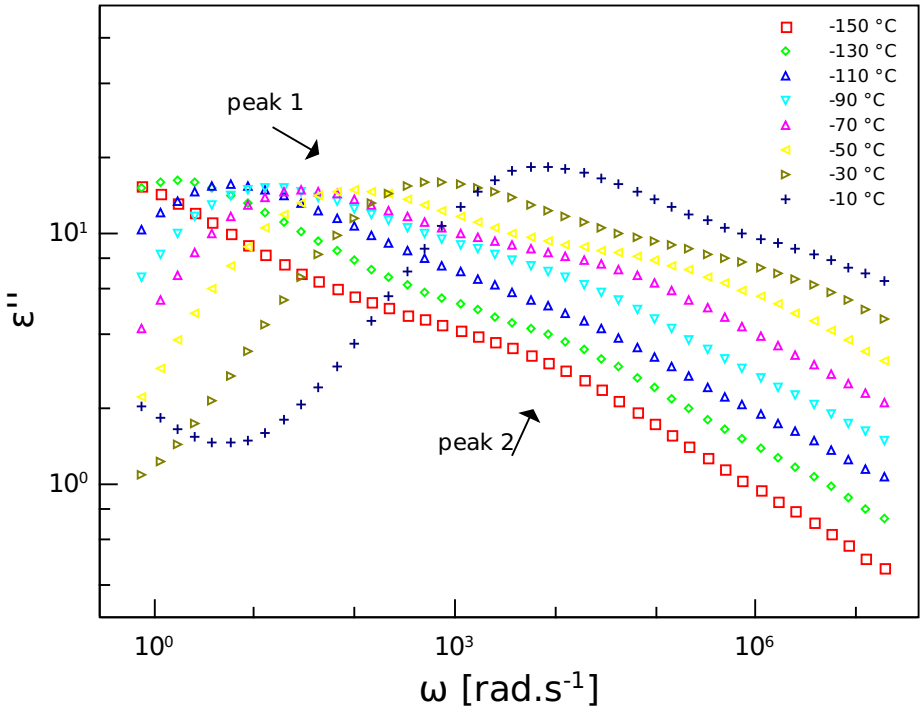

Figure 4.29: A dielectric spectrum of PANI/MMT(CL) B5, ϵ'' plot.

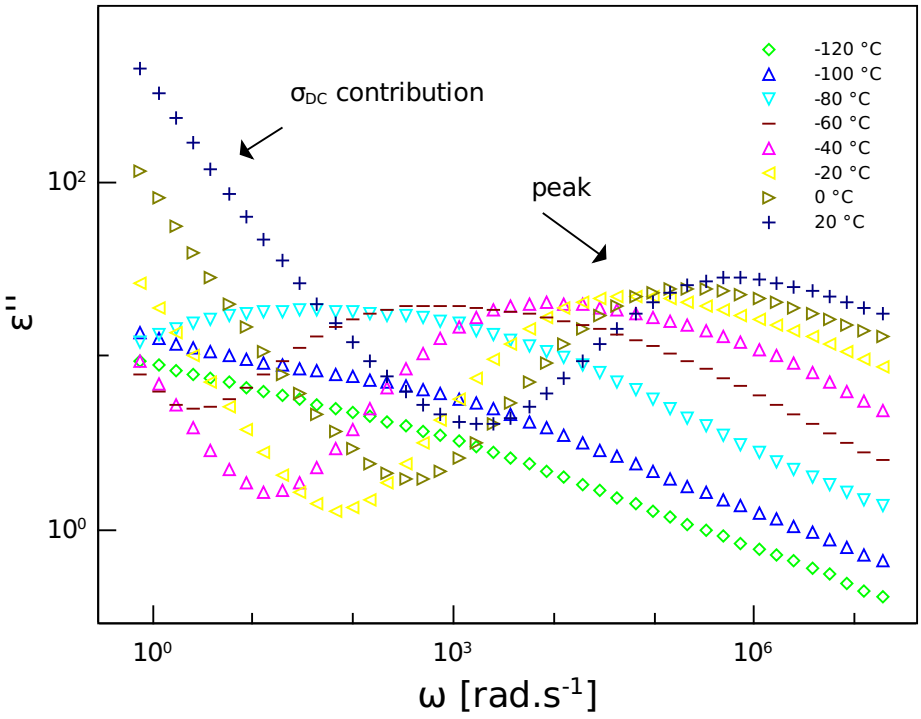

Figure 4.30: A dielectric spectrum of PANI/MMT(BF) B5, ϵ'' plot.

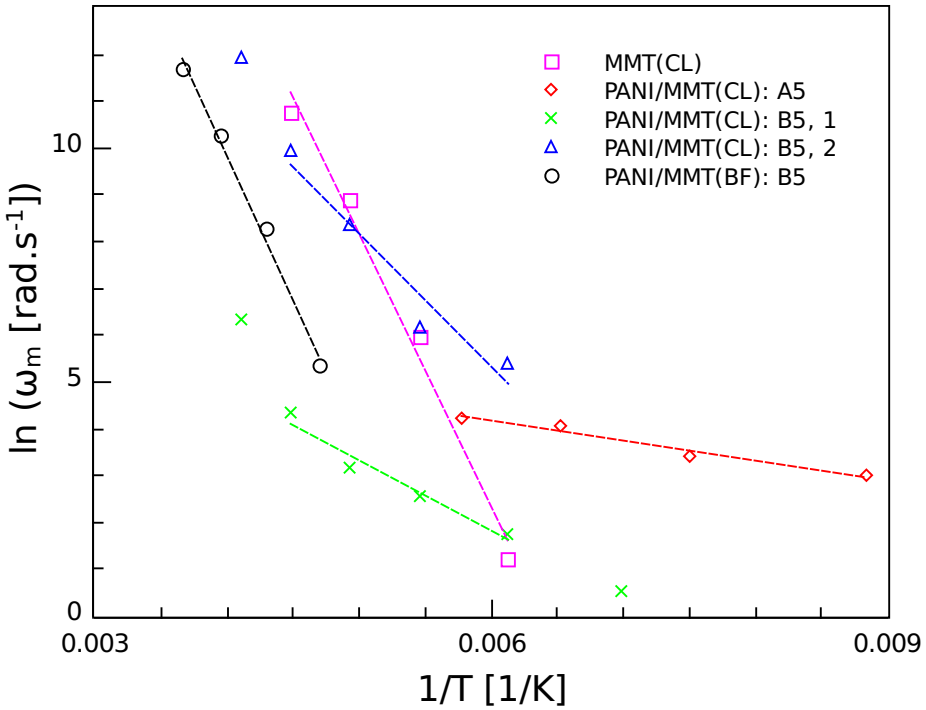

Figure 4.31: A temperature shift in the frequency maximum fitted by the Arrhenius equation.

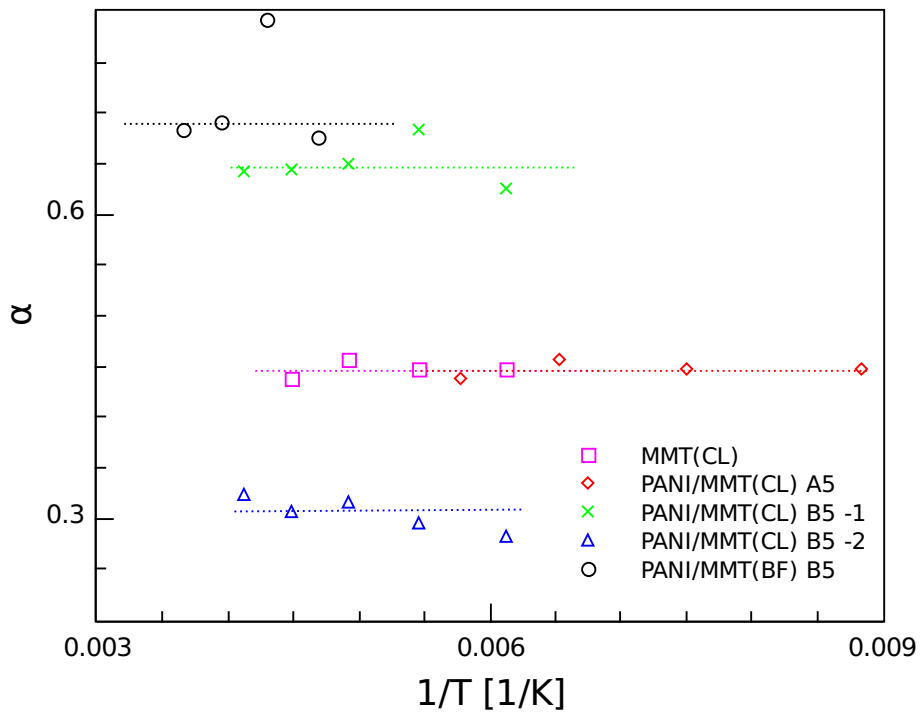

Figure 4.32: The parameter α of the Cole-Cole equation obtained from a fitting procedure. The lines are guides for the eyes only.

An identification of the dielectric losses origin is rather a difficult task since the structure of PANI/MMT composites is very complex. There are cations of sodium in MMT which contribute to the dielectric response [64], or in composites there could be residual aniline cations acting similarly. Water molecules probably play a role as well. Finally, a local movement of the polymer chains (or their parts) and different interactions between dopant anions, silica layers and so on may be other 'source' of the polarisation. The dielectric spectroscopy thus can give an interesting and a valuable piece of information about the structure and the processes in materials but in order to gain a maximum, for these conducting and very complex materials following approaches are mainly useful: a lower working temperature range to minimise effect of the σ_{DC} conductivity as much as possible, and a usage of the different technique such as the thermally stimulated depolarization currents technique. This is however leading to further and more robust investigation which lies far away from the scope of this thesis.

4.2.6 Conclusions

In this part of the work we have investigated the electrical properties of PANI/MMT composites. Both, σ_{DC} and σ_{AC} were of our interest and different methods for their investigations were used. In general, composites are semiconducting materials and their room temperature conductivity varies within six orders of magnitude, at least

for the 'VdP conductivity', in respect to amount of insulating matrix MMT. Due to failure of the classical percolation dependence it deserves more attention to determine the threshold more precisely (if possible) what can be useful mainly in possible applications. Nevertheless, it seems that less than 40 w.t.% (50 vol.%) of PANI is needed to achieve the conductive composite with similar properties as pure PANI shows. The effect of ageing is not drastic but is bigger that for PANI what is not a good point for composites.

The charge transport in this complex system seems to be dominated by PANI because composites show the similar temperature dependences and MMT rather plays a role of an insulating medium. A superposition of the Q1D VRH and the Arrhenius-like transport was successfully fitted with parameters reflecting an increase in barriers with the higher amount of MMT in agreement with literature. But the rest of models is not strictly excluded. The leading role of PANI in the conductivity is also reflected in the time dependences at low pressure which are similar to the pure PANI characteristics.

The nature of disordered solids is confirmed in composites by the AC characteristics with a typical low frequency plateau and usually a very good agreement with the DC values. An increase at higher frequencies was also observed. It can be described in the frame of the phenomenological 'universal' law but unfortunately without any satisfactory specification to the microscopic model (such as the random free energy barriers model) neither for the aged samples nor for the original ones where even the 'universal' law fails in terms of the exponent s higher than one. Apart of this one has to face a lot of experimental issues. Thus a wider investigation is still needed in order to gain from the AC conductivity phenomenon.

The differences at least in one order of magnitude (but up to three for original samples) were observed for two different methods. As it is believed both measure the bulk conductivity, an anisotropy of conductivity is suggested with the lower values for direction perpendicular to the surface.

An influence of three parameters in the preparation procedure was investigated. The only one important seems to be the content of MMT in reaction mixture since the rest - the different polymerisation process and the origin of MMT does not significantly influence the final electrical properties.

Again, this area of research still offers further investigation, mainly in the AC conductivity and the dielectric spectroscopy, the anisotropy or the percolation threshold 'hunting'. Despite of the lack of any superiority in the electric properties, these composites still provide a fine PANI-like behaviour and together with enhanced other properties (e.g. mechanical, processability) could be used in applications.

Chapter 5

Conclusions

In the presented thesis two conducting polymer-based systems were studied, in the concrete, polyaniline-silver composites and polyaniline-montmorillonite composites. Several experimental techniques and devices were used to obtain the AC and the DC characteristics of samples at a room temperature and also their temperature dependences. Also a discussion of the ageing effect was done. All characteristics were studied in respect to the different preparation conditions such as doping acids and their molar concentration in the case of polyaniline-silver composites or the origin of montomorillonite, its content in compounds and the polymerisation process in the case of polyaniline-montmorillonite composites. A confrontation of the experimental data with known theoretical models was performed where possible.

All results, discussions, conclusions and outlooks were in details presented in chapter 4 but the main results coming from our investigation are:

- Polyaniline-silver composites - a very diversform behaviour was observed within different dopants and their concentration used, from the semiconducting to the metallic behaviour with the room temperature conductivity variation $10^{-2} - 10^{3}$ S/cm and the relative change in vacuum from almost 40% drop through the independence to the increase. The composites were found to be stable in terms of the ageing since their room temperature conductivity decrease in 2 years is less than 10%. From a structural point of view the fluctuation-induced tunnelling model was preferred within measured temperature range, however a superposition of the charge energy limited tunneling and the Arrhenius-like thermally activated process transport was not strictly excluded.
- Polyaniline-montmorillonite composites - the semiconducting behaviour similar to pure PANI was observed but with the strong dependence on MMT content and variation of the conductivity within $10^{-6} - 10^{0}$. Less than 40 w.t.% was needed to obtain values similar to PANI and only of a slightly worse time stability. The transport mechanism was attributed mainly to PANI and a super-

position of the quasi-one dimensional variable hopping and the Arrhenius-like thermally activated process was suggested to cover the investigated temperature range. It is believed MMT increases a disorder in composite. Also possible anisotropy in the conductivity was observed with the differences at least one order of magnitude. The AC conductivity confirmed the disorder nature of a material but up to now without a clear relation to any microscopic model. One or two relaxation mechanisms described by the Cole-Cole function were revealed by the dielectric spectroscopy for less conductive samples. Any considerable differences in the electrical properties in respect to the origin of MMT or to the polymerisation ways were not found.

Bibliography

[1] Heeger A.J. Semiconducting and metallic polymers: The fourth generation of polymeric materials. *Rev. Mod. Phys.*, 73(3):681–700, 2001.

[2] Kaiser A.B. Electronic properties of conducting polymers and carbon nanotubes. *Rep. Prog. Phys.*, 64:1–49, 2001.

[3] Roth S. *One-dimensional metals*. VCH, Weinheim, 1995. ISBN 3–527–26875–8.

[4] Schönhals A. and Kremer F. Theory of dielectric relaxation. In Kremer F. and Schönhals A., editors, *Broadband dielectric spectroscopy*, chapter 1. Springer, 2003. ISBN 3–540–43407–0.

[5] Chambers R.G. *Electrons in metals and semiconductors*. Chapman and Hall, 1990. ISBN 0–412–36840–4.

[6] Hamman C. et al. *Electrical conduction mechanisms in solids*. VEB Deutscher Verlag der Wissenschaften, Berlin, 1988. ISBN 3–326–00380–3.

[7] Heeger A.J. et al. Solitons in conducting polymers. *Rev. Mod. Phys.*, 60:782–851, 1988.

[8] Bernier P. et al., editor. *Advances in synthetic metals. Twenty years of progress in science and technology.* Elsevier, 1999. ISBN 0–444–72004–9.

[9] McGehee M.D. et al. Twenty years of conducting polymers: From fundamental science to applications. In Bernier P. et al., editor, *Advances in synthetic metals. Twenty years of progress in science and technology.*, chapter 2. Elsevier, 1999.

[10] Krempasky J. et al. *Synergetika*. Vydavateľstvo Slovenskej Akadémie Vied, Bratislava, 1988.

[11] Pietronero L. Ideal conductivity of carbon π polymers and intercalation compounds. *Synthetic Metals*, 8:225–231, 1983.

[12] Mott N.F. Conduction in non-crystalline materials. Localized states in a pseudogap and near extremities of conduction and valence bands. *Phil. Mag.*, 19(160):835–852, 1969.

[13] Efros A.L. and Shklovskii B.I. Coulomb gap and low temperature conductivity of disordered systems. *J. Phys. C*, 8:L49–L51, 1975.

[14] Fogler M.M. et al. Variable-range hopping in quasi-one-dimensional electron crystals. *Phys. Rew. B*, 69, 2004.

[15] Sheng P. et al. Hopping conductivity in granular metals. *Physical Review Letters*, 31(1):44–47, 1973.

[16] Sheng P. Fluctuation-induced tunneling conduction in disordered materials. *Physical Review B*, 21(6):2180–2195, 1980.

[17] Sheng P. and Klafter J. Hopping conductivity in granular disordered systems. *Physical Review B*, 27(4):2583–2586, 1983.

[18] Zuppiroli L. et al. Hopping in disordered conducting polymers. *Physical Review B*, 50(8):5196–5203, 1994.

[19] Travers J.P. et al. Is granularity the determining feature for electron transport in conducting polymers? *Synthetic Metals*, 101:359–362, 1999.

[20] Stauffer D. *Introduction to percolation theory.* Taylor and Francis, 1985. ISBN 0–85066–315–6.

[21] Knackstedt A.M. and Roberts A.P. Morphology and macroscopic properties of conducting polymer blends. *Macromolecules*, 29:1369–1371, 1996.

[22] Webman I. et al. Critical exponents for percolation conductivity in resistor networks. *Phys. Rew. B*, 16:2593–2596, 1997.

[23] Toker D. et al. Tunneling and percolation in metal-insulator composite materials. *Phys. Rew. B*, 68, 2003.

[24] Dyre J.C. The random free-energy barrier model for ac conductivity in disordered solids. *J. Appl. Phys.*, 64:2456–2468, 1988.

[25] Long A.R. Frequency-dependent loss in amorphous semiconductors. *Advances in Physics*, 31, 1982.

[26] Elliott S.R. A.c. conduction in amorphous chalcogenide and pnictide semiconductors. *Advances in Physics*, 36:135–218, 1987.

[27] Dyre J. and Schröder T.B. Universality of ac conduction in disordered solids. *Reviews of Modern Physics*, 72:873–892, 2000.

[28] Dyre J. et al. Fundamental questions relating to ion conduction in disordered solids. *Rep. Prog. Phys.*, 72:873–892, 2009.

[29] Kremer F. and Rozanski S.A. The dielectric properties of semiconducting disordered materials. In Kremer F. and Schönhals A., editors, *Broadband dielectric spectroscopy*, chapter 12. Springer, 2003. ISBN 3–540–43407–0.

[30] Bianchi R.F. et al. Alternating current conductivity of polyaniline. *J. Chem. Phys.*, 110:4062–4607, 1999.

[31] Schönhals A. and Kremer F. Analysis of dielectric spectra. In Kremer F. and Schönhals A., editors, *Broadband dielectric spectroscopy*, chapter 3. Springer, 2003. ISBN 3–540–43407–0.

[32] Schönhals A. Molecular dynamics in polymer model systems. In Kremer F. and Schönhals A., editors, *Broadband dielectric spectroscopy*, chapter 7. Springer, 2003. ISBN 3–540–43407–0.

[33] Marsitzky D. and Müllen K. 20 years of synthetic metals the role of synthesis. In Bernier P. et al., editor, *Advances in synthetic metals. Twenty years of progress in science and technology.*, chapter 1. Elsevier, 1999.

[34] MacDiarmid A.G. and Epstein A.J. Polyanilines: A novel class of conducting polymers. *Faraday Discuss. Chem. Soc.*, 88:317–332, 1989.

[35] Konyushenko E.N. et al. Polyaniline nanotubes: Conditions of formation. *Polymer Int.*, 55:31–39, 2006.

[36] Bober P. et al. Conducting polyaniline-montmorillonite composites. *Syntetic Metals*, 160:2596–2604, 2010.

[37] Runt J.P. and Fitzgerald J.J:, editors. *Dielectric spectroscopy of polymeric materials*. American chemical society, Washington, 1997. ISBN 0–8412–3335–7.

[38] Pauw L.J. van der. A method of measuring specific resistivity and hall effect of discs of arbitrary shape. *Philips Res. Repts*, 13:1–9, 1958.

[39] Schroder D.K. *Semiconductor material and device characterization*. John Wiley and sons, New York, 1998. ISBN 0–471–24139–3.

[40] Honda M. *The impedance measurement handbook. A guide to measurement technology and techniques*. Yokogawa-Hewlett-Packard, Tokyo, 1989.

[41] Novocontrol Technologies, Hundsangen. *Alpha and beta dielectric, conductivity, impedance and gain phase analyzers*, 2005.

[42] Bober P. et al. Polyaniline-silver composites prepared by the oxidation of aniline with silver nitrate in solutions of sulfonic acids. *Electrochim. Acta*, 56(10):3580–3585, 2010.

[43] Blinova N. V. et al. Polyaniline-silver composites prepared by the oxidation of aniline with silver nitrate in acetic acid solutions. *Polym.Int.*, 59:437–446, 2010.

[44] Silver mineral data. Available online at URL: `http://webmineral.com/data/Silver.shtml`. [cit. 2011-04-13].

[45] Kharoo H.L. et al. Phonon-limited electrical and thermal resistivities of noble metals. *Phys. Rew. B*, 18(10):5419–5426, 1977.

[46] Smith D.R. and Fickett F.R. Low-temperature properties of silver. *J. Res. Natl. Inst. Stand. Technol.*, 100(2):119–171, 1995.

[47] Stejskal J. et al. The reduction of silver ions with polyaniline: The effect of type of polyaniline and the mole ratio of the reagents. *Material Letters*, 63:709–711, 2009.

[48] Ye L. et al. Effect of Ag particle size on electrical conductivity of isotropically conductive adhesives. *IEEE transactions on electronics packaging manufacturing*, 22(4):299–302, 1999.

[49] Stejskal J. Personal communication, 2011. the Institute of Macromolecular Chemistry of Academy of Sciencies of the Czech Republic, Heyrovského nám. 2, Prague.

[50] Kuphaldt T.R. Lessons in electric circuits. Available online at URL: `http://www.opamp-electronics.com/tutorials/temperature_coefficient_of_resistance_1_12_06.htm`, 2002. [cit. 2011-04-11].

[51] Joo J. et al. Microwave dielectric response of mesoscopic metallic regions and the intrinsic metallic state of polyaniline. *Phys. Rew. B*, 49(4):2977–2980, 1994.

[52] Pinto N.J. et al. Conducting state of pani films. *Physical Review B*, 53(16):10690–10694, 1996.

[53] Wolter A. et al. Model for aging in HCl-protonated polyaniline: Structure, conductivity, and compostition studies. *Phys. Rew. B*, 58(12):7638–7647, 1998.

[54] Zaarei D. et al. Structure, properties and corrosion resistivity of polymeric nanocomposite coatings based on layered silicates. *J. Coat. Technol. Res.*, 5:241–249, 2008.

[55] Salahuddin N. et al. Synthesis and characterization of polyaniline-organoclay nanocomposites. *J. of Applied Polymer Science*, 107:1981–1989, 2008.

[56] Song D.H. et al. Intercalated conducting polyaniline-clay nanocompositesand their electrical characteristics. *J. of Chem. and Phys. of Solids*, 69:1383–1385, 2008.

[57] Krishantha D.M.M. et al. Ac impedance analysis of polyaniline-montmorillonite nanocomposites. *Ionics*, 12:287–294, 2006.

[58] Kim B.H. et al. Nanocomposite of polyaniline and Na^+-montmorillonite clay. *Macromolecules*, 35:1419–1423, 2002.

[59] Lee D. et al. Structural changes of polyaniline/montmorillonite nanocomposites and their effects on physical properties. *J. Mater. Chem.*, 13:2942–2947, 2003.

[60] Ishida T. et al. Dielectric-relaxation spectroscopy of kaolinite, montmorillonite, allophane, and imogolite under moist conditions. *Clays and Clay Minerals*, 48(1):75–84, 2000.

[61] Rizvi T.Z and Shakoor A. Electrical conductivity and dielectric properties of polypyrrole/Na^+montmorillonite (PPy/Na^+-MMT)clay nanocomposites. *J. Phys. D*, 42, 2009.

[62] Kremer F. and Schönhals A., editors. *Broadband dielectric spectroscopy.* Springer, 2003. ISBN 3–540–43407–0.

[63] Papathanassiou A.N. et. al. Universal frequency-dependent ac conductivity of conducting polymer networks. *App. Phys. Lett.*, 91, 2007.

[64] Haouzi A. et. al. Activation energy for dc conductivity in dehydrated alkali metal-exchanged montmorillonites: Experimental results and model. *Applied Clay Science*, 27:67–74, 2004.